

HOSTED BY



ELSEVIER

Contents lists available at ScienceDirect

China University of Geosciences (Beijing)

Geoscience Frontiers

journal homepage: www.elsevier.com/locate/gsf

Research Paper

Evolution of Siderian juvenile crust to Rhyacian high Ba-Sr magmatism in the Mineiro Belt, southern São Francisco Craton

Hugo Moreira^{a,*}, Luís Seixas^b, Craig Storey^a, Mike Fowler^a, Stephanie Lasalle^a,
Ross Stevenson^c, Cristiano Lana^b

^a School of Earth and Environmental Sciences, University of Portsmouth, Burnaby Building, Burnaby Road, Portsmouth, PO1 3QL, UK

^b Departamento de Geologia, Escola de Minas, Universidade Federal de Ouro Preto, Ouro Preto, MG 35400-000, Brazil

^c GEOTOP Université du Québec à Montréal, P.O. Box 8888, Station Centre Ville, Montréal, Québec H3C 3P8, Canada



ARTICLE INFO

Article history:

Received 4 September 2017

Received in revised form

29 November 2017

Accepted 25 January 2018

Available online 20 February 2018

Keywords:

São Francisco Craton

Magmatic lull

TTG–Sanukitoid transition

Zircon U–Pb–Hf

Titanite U–Pb

Whole rock Nd isotopes

ABSTRACT

Plutonic rocks from the Mineiro Belt, Brazil record a delayed onset of the transition from TTG to sanukitoid-type magmatism (high Ba-Sr), starting during the Siderian magmatic lull when little juvenile magma was added to the continental crust. Rocks mostly belong to the calc-alkaline series, meta- to peraluminous and originally “I-type”, meaning that oxidized magmas were formed by partial melting of subducted material. The temporal distribution and apparent secular changes of the magmas are consistent with the onset of subduction-driven plate tectonics due to an increase of the subduction angle and opening of the mantle wedge. New isotopic analyses (Sm–Nd whole rock and Lu–Hf in zircon) corroborate the restricted juvenile nature of the Mineiro Belt and confirm the genetic link between the Lagoa Dourada Suite, a rare ca. 2350 Ma high-Al tonalite-trondhjemitic magmatic event, and the sanukitoid-type ca. 2130 Ma Alto Maranhão Suite. U–Pb dating of zircon and titanite constrain the crystallisation history of plutonic bodies; coupled with major and trace element analyses of the host rocks, they distinguish evolutionary trends in the Mineiro Belt. Several plutons in the region have ages close to 2130 Ma but are distinguished by the lower concentration of compatible elements in the juvenile high Ba-Sr suite.

© 2018, China University of Geosciences (Beijing) and Peking University. Production and hosting by Elsevier B.V. This is an open access article under the CC BY-NC-ND license (<http://creativecommons.org/licenses/by-nc-nd/4.0/>).

1. Introduction

Understanding the secular evolution of the continental crust and the onset of subduction-driven tectonics has been based on analytical experiments, modelling and/or field relationships (Stern, 2005, 2016; Condie and Pease, 2008; Korenaga, 2013; Moore and Webb, 2013; Gerya et al., 2015; Roberts and Spencer, 2015; Smart et al., 2016). Even so, the matter of when and how plate tectonics begun is still heavily debated (Moyen et al., 2006; Cawood et al., 2009; Arndt and Davaille, 2013; Hawkesworth et al., 2016; Smart et al., 2016; Stern et al., 2016, 2017; Ernst, 2017; Rozel et al., 2017). Proponents of plate tectonics beginning in the Archean (e.g. Dhuime et al., 2012; Cawood et al., 2013; Condie, 2016) agree on two points: (1) most of the crust had been produced by the end

of the Archean; (2) subduction-driven plate tectonics is a gradual and evolving mechanism, which started at ca. 3.0 Ga and evolved to a modern style by ca. 2.5 Ga. A secular geochemical transition in arc-related magmas reflects the second observation, where the opening of the mantle wedge after a period of shallower subduction promoted interaction between metasomatised mantle and crustal derived magmas (Martin and Moyen, 2002; Martin et al., 2010). Globally, this tectonic change is recorded by a geochemical transition starting with Tonalite-Trondhjemitic-Granodiorite (TTG) magmas dominantly produced during the Palaeoarchean. Processes gradually evolved from ca. 3.0 Ga towards sanukitoids (high Ba-Sr), in places accompanied by hybrid granitoids (Shirey and Hanson, 1984; Laurent et al., 2014) at 2.5 Ga.

The subsequent scenario of Earth's geodynamics was marked by an apparent “global magmatic shutdown”, also referred to as the Siderian Quiet Interval (2.45–2.20 Ga; e.g. Condie et al., 2009; Pehrsson et al., 2014) or the presently-preferred terminology “magmatic lull” (Stern et al., 2017). Lithospheric stagnation is proposed to explain this period of little addition of juvenile magmas to

* Corresponding author.

E-mail address: hugo.moreira@port.ac.uk (H. Moreira).

Peer-review under responsibility of China University of Geosciences (Beijing).

the continental crust, and is recorded as a temporal hiatus within large datasets of magmatic and detrital zircon ages (O'Neill et al., 2007; Condie et al., 2009). However, the notion of a shutdown of plate tectonics is increasingly questioned due to documentation of many rock types within the proposed interval (for a recent review see Partin et al., 2014). The perceived lack of data is attributed either to sampling bias or a geological response to supercontinent assembly. In the second option, the amalgamation of the first supercontinent possessing margins akin to current continents (Flament et al., 2008), named Kenorland (Williams et al., 1991), shortened the cumulative length of active subduction zones and, therefore, reduced magmatic activity (Silver and Behn, 2008; Pehrsson et al., 2014).

Recent studies in the Mineiro Belt, southern Brazil, reported important occurrences of plutonic igneous rocks that fit in the aforementioned time gap (e.g. Seixas et al., 2012; Teixeira et al., 2015). They describe the Lagoa Dourada and Resende Costa TTG juvenile suites in the southern portion of the São Francisco Craton (SSFC), dated at ca. 2.35–2.30 Ga (Fig. 1a–c). The region also contains other juvenile (I-type) magmatic arcs, named the Serrinha-Tiradentes (ca. 2.22 Ga) and Alto Maranhão (ca. 2.13 Ga) suites (Seixas et al., 2013; Ávila et al., 2014). The Alto Maranhão Suite is geochemically similar to late Archaean, mantle-derived sanukitoids (Seixas et al., 2013).

Fig. 2 compiles U-Pb-Hf zircon analyses from the SSFC. Igneous zircons are divided by different granitoid types based on published petrogenetic classification (yellow for TTG, pink for hybrid and purple for sanukitoid). Those granitoid types, corresponding to TTG and hybrid sources, were formed during two time intervals, whereas sanukitoids only formed during one of these. There is a late TTG to sanukitoid transition starting during the magmatic lull, indicated in red. Thus, a temporal shift is registered in the secular geochemical evolution of arc-related magmas straddling the Archaean to Palaeoproterozoic (e.g. Halla et al., 2017).

Major and trace element studies of several granitoids in the region expand the geochemical dataset from the Mineiro Belt. Major, trace and Rare Earth Elements (REE) are used to document the transition from TTGs to sanukitoid and hybrid granitoids. U-Pb analyses of accessory zircon and titanite and whole rock Sm-Nd and in-situ zircon Lu-Hf isotopic analyses are used to constrain the crustal sources and isotopic evolution of the Mineiro Belt.

2. Geological background and rationale

The São Francisco Craton consists of Archaean and Palaeoproterozoic crustal segments, initially assembled in the Palaeoproterozoic era, and best exposed in its northern and southern domains. Its counterpart is located in the Congo Craton in central West Africa (e.g. Alkmim and Marshak, 1998; Teixeira et al., 2015, 2017a,b; Aguilar Gil et al., 2017) (Fig. 1a). Collisional processes involved recycling and melting of the Archaean crust during a protracted high grade metamorphic overprint from ca. 2.10 Ga to 1.94 Ga. The Palaeoproterozoic belt is evidence of these processes and is known as the Minas Orogen (Teixeira et al., 2017a) and by various temporally related occurrences in the interior of the SSFC (Barbosa and Sabaté, 2004; Peucat et al., 2011; Carvalho et al., 2016, 2017; Aguilar Gil et al., 2017; Alkmim and Teixeira, 2017; Teixeira et al., 2017b). The Archaean basement of the southern portion of the craton, the Quadrilátero Ferrífero (QF), is composed of TTGs, which range in age from 3.20 Ga to 2.76 Ga, later intruded by transitional medium-K to high-K granitoids between 2.76 Ga and 2.63 Ga (Carneiro, 1992; Lana et al., 2013; Romano et al., 2013; Farina et al., 2015, 2016; Moreno et al., 2017) (Fig. 1b). In addition, Farina et al. (2015) revealed that the previously assumed TTGs also had a contribution of melts derived from continental crust in their

genesis (not solely derived from partial melting of mafic oceanic crust – Moyen and Martin, 2012). Similarly, K-granitoids were formed from the melting of TTGs and also from low-degree partial melting of metagreywacke. These arguments are based on detailed geochemical comparison of basement rocks of the QF with experimental melts produced by partial melting of TTGs. Indeed, the geochemical and geochronological evolution of the basement is also temporally related to the deposition and closure of a typical metavolcanoclastic greenstone belt basin, known as Rio das Velhas Supergroup, in which metagreywackes were formed (Dorr, 1969; Noce et al., 2005; Baltazar and Zucchetti, 2007; Lobato et al., 2007; Moreira et al., 2016). Moreover, recent combined U-Pb, Lu-Hf and O isotopes on single zircons demonstrated that Archaean segments are distinct, presenting individual evolutionary trends and confirming the presence of metasediments in the petrogenesis of Neoproterozoic high-K granitoids (Albert et al., 2016). However, the absence of sanukitoid magmas that make the link between TTGs to calc-alkaline transition is different from Archaean cratonic lithosphere worldwide (Laurent et al., 2014; Halla et al., 2017) (Fig. 2). Farina et al. (2015) first reported this deficiency in a thorough geochemical study of three main granite-gneissic complexes in the region, the Bação, Bonfim and Belo Horizonte complexes of the SSFC (Fig. 1b). This deficiency casts doubt on models of continental subduction during the Meso- to Neoproterozoic in the region. A lack of sanukitoid magmas raises the question of when and if it occurred. This is one of the major questions in understanding the evolutionary history of Archaean crust in the SSFC.

Significantly, the emplacement of potassic magmas in SSFC led to the stabilization of the Archaean crust (Romano et al., 2013). Heat-producing elements (e.g. K, Th and U) extracted from the deep crust during partial melting of older crust subsequently partitioned into granite magmas (Taylor and McLennan, 1985; Romano et al., 2013). The concentration of such elements in the upper crust is one of the possibilities that led to thermal stability, providing conditions suitable for the accumulation of the eventual kilometre-thick column of sediments, and so the lower crust became refractory and resistant to subsequent melting (e.g., Sandiford et al., 2002). This sedimentation is represented in the SSFC by the 8000 m-thick Minas Supergroup, an intracratonic rift basin which opened shortly after cratonic stabilization (after 2.60 Ga) and closed around 2.12 Ga with the deposition of the syn-orogenic Sabará Group (Machado et al., 1996; Hartmann et al., 2006; Martínez Dopico et al., 2017) (Fig. 2). The Minas basin contains large Lake Superior-type banded iron formation and a world-class iron deposit, the Cauê Formation (Dorr, 1969; Rosière et al., 2008).

The Minas Supergroup is unconformably overlain by the Itacolomi Group, deposited after 2.059 Ga (Machado et al., 1996). The inversion and subsequent closure of the Minas basin was caused by the Palaeoproterozoic orogeny, divided into three main plutonic belts that together characterize a long-lived system of oceanic and continental magmatic arcs (Teixeira et al., 2015, 2017a; Alkmim and Teixeira, 2017) (Fig. 1b): (1) Mineiro Belt (focus of this study), (2) Mantiqueira Belt, and (3) Juiz de Fora Belt. The last two belts comprise respectively a Cordilleran-type adjoining terrane emplaced between 2.17 Ga and 2.0 Ga with Archaean inheritance, and an outermost juvenile-type terrane accreted from 2.20 Ga to 2.0 Ga. The Palaeoproterozoic suture between these two belts, the Abre Campo shear zone, was formed during the late Neoproterozoic Araçuaí orogeny, which also strongly deformed and metamorphosed both terranes (Alkmim and Noce, 2006; Heilbron et al., 2010) (Fig. 1a and b).

In contrast to the Mantiqueira and Juiz de Fora domains, the Mineiro Belt was shielded from the Neoproterozoic overprint and its plutonic suites range in age from 2.47 Ga to 2.0 Ga (Ávila et al., 2010, 2014; Barbosa et al., 2015; Teixeira et al., 2015, 2017a). The belt comprises an area larger than 6000 km² bounded to the north

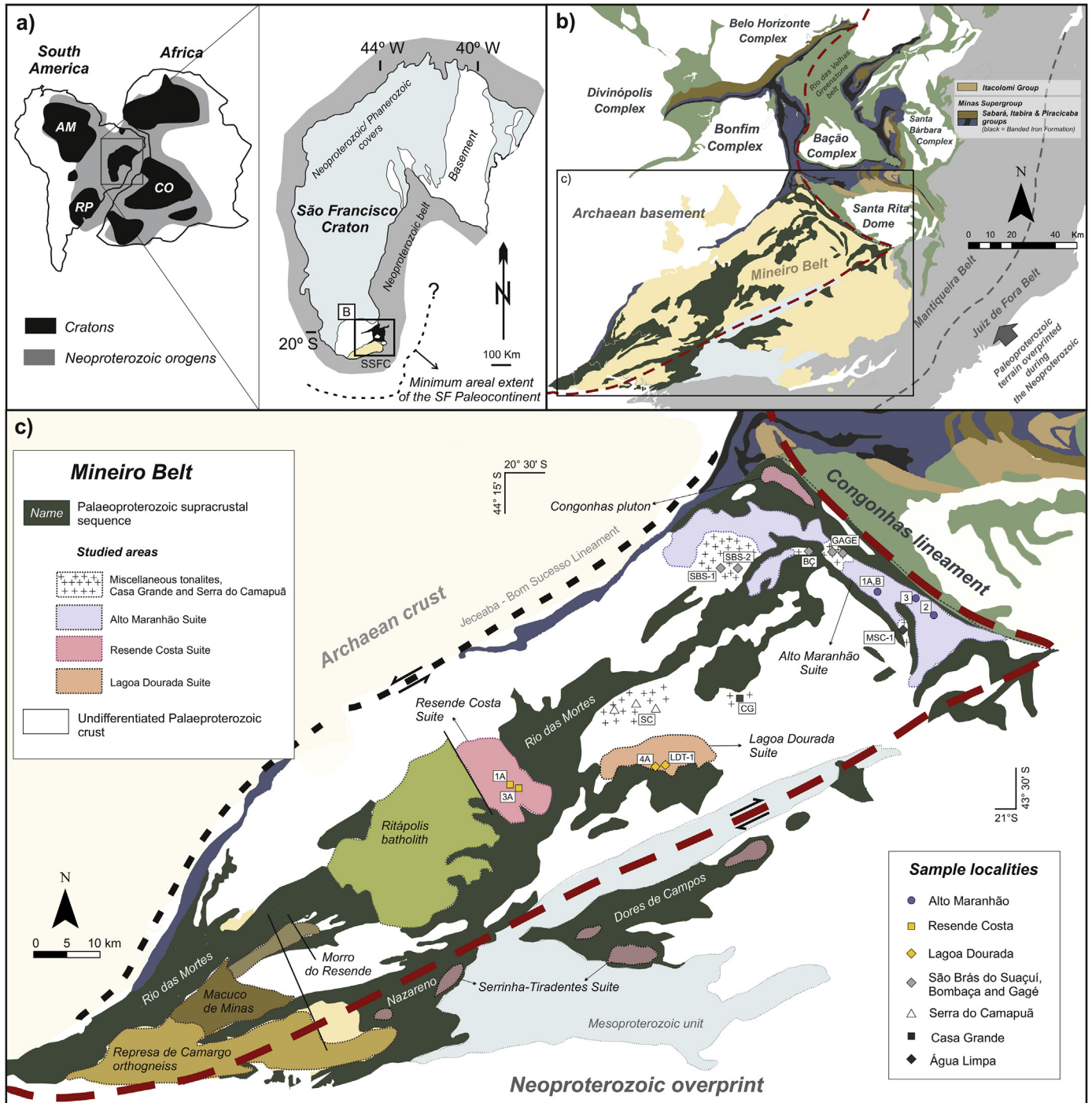


Figure 1. Geological settings of the São Francisco Craton and its southern margin. (a) Cratons and Neoproterozoic orogens of South America and Africa in West Gondwana. São Francisco Craton and the Neoproterozoic margins. Quadrilátero Ferrífero (QF) is situated in the southern domain of the craton where Archean crust is exposed (modified from Heilbron et al., 2010; Alkmim and Martins-Neto, 2012). (b) Southern São Francisco Craton and possible boundary along principal belts during the Minas accretionary orogeny and later Neoproterozoic belt (modified from Heilbron et al., 2010; Alkmim and Martins-Neto, 2012; Teixeira et al., 2015). Grey dashed line is the Abre Campo shear zone, which defines the contact between Juiz de Fora and Mantiqueira belts. Red dashed line is current craton boundary. (c) Geological map of Mineiro Belt indicating principal domains and lithologies of the region (modified from Seixas et al., 2013; Barbosa et al., 2015).

by the NE–SW Jeceaba-Bom Sucesso Lineament, to the east by the NW–SE Congonhas Lineament and to the south by a Palaeoproterozoic high-grade metamorphic terrane that contains zircons with Archean cores (Noce et al., 2007) (Fig. 1b). The NE–SW and NW–SE lineaments are major boundaries between the Mineiro Belt and the Archean continental margin of the proto-São Francisco Craton (e.g., Teixeira et al., 2015) (Fig. 1c).

Another important difference is that the Mineiro belt is essentially composed of juvenile granitoids (discussed below) intruded by later phases with different degrees of crustal contamination/assimilation (e.g., Ávila et al., 2010, 2014; Seixas et al., 2012, 2013; Barbosa et al., 2015; Teixeira et al., 2015). The mantle signature is given by Lu-Hf and Sm-Nd analyses, in single zircons or whole rock, correspondingly. Locally, xenoliths and roof pendants of

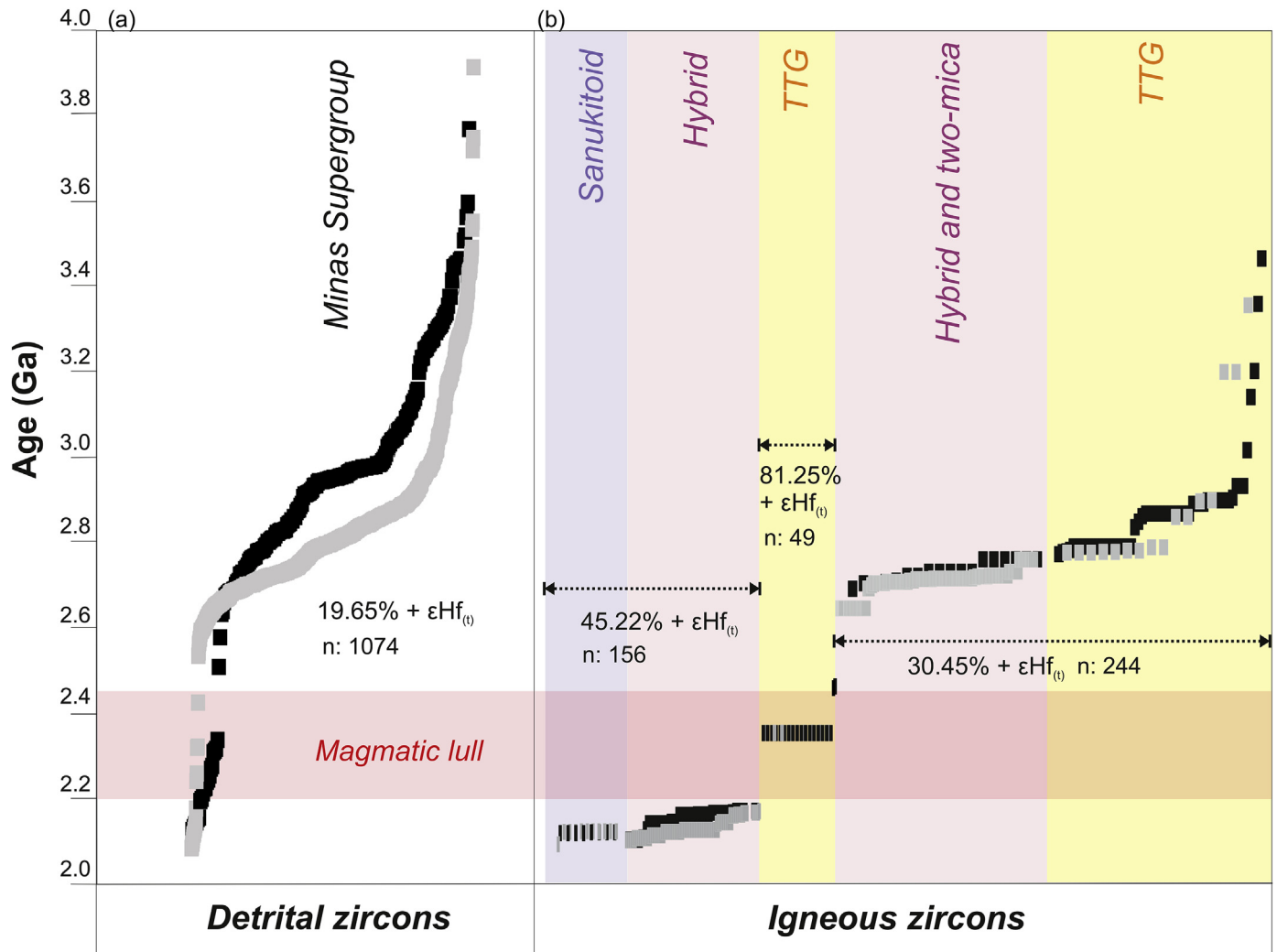


Figure 2. Compilation of U-Pb-Hf zircon analyses of (a) the Minas Basin containing zircon data ranging in age from ca. 3.9 Ga to 2.1 Ga (Martínez Dopico et al., 2017) and (b) igneous zircon ages from both Archaean domains within the QF (Albert et al., 2016) and the Palaeoproterozoic Mineiro Belt (Barbosa et al., 2015; Teixeira et al., 2015; this study); positive $\epsilon_{\text{Hf}}(t)$ values are black, negative are grey. Positive $\epsilon_{\text{Hf}}(t)$ percentage is indicated in specific intervals. Red interval corresponds to the magmatic lull.

amphibolite are found (Ávila et al., 2010; Seixas et al., 2012, 2013). The supracrustal rocks surrounding the granitoids are carbonaceous phyllites, gondites, quartzites, metagreywackes and tholeiitic-komatiitic metavolcanic rocks (Ávila et al., 2010, 2014). Metavolcanic-sedimentary sequences are subordinate (for a recent review see Alkmim and Teixeira, 2017). Amphibolites and metavolcanics have variable source isotope signatures ($\epsilon_{\text{Nd}}(t)$: -15.9 to $+6.1$; Ávila et al., 2010, 2014; Teixeira et al., 2015) and U-Pb ages between 2.1 and 2.3 Ga with older Archaean contributions (2.8 and 2.9 Ga). Older supracrustal sequences (ca. 2.3 Ga) were later intruded by plutonic bodies (2.1 Ga) (Toledo, 2002; Teixeira et al., 2008, 2015; Ávila et al., 2014; Barbosa et al., 2015). Table 1 summarizes the main plutonic occurrences studied so far in the Mineiro Belt, together with U-Pb ages of zircons and also the published $\epsilon_{\text{Hf}}(t)$ and $\epsilon_{\text{Nd}}(t)$ data. Among them, we draw attention here to the Lagoa Dourada, Resende Costa Orthogneiss, Serrinha-Tiradentes and Alto Maranhão suites (Seixas et al., 2012, 2013; Ávila et al., 2014; Teixeira et al., 2015).

3. Petrogenetic significance of plutonic rocks in the Mineiro Belt

The Lagoa Dourada Suite is the first record of Siderian magmatism within the Mineiro Belt (crystallisation age of

2349 ± 4 Ma, Seixas et al., 2012). The suite consists of a low-K, high Al_2O_3 and low Mg# juvenile TTG-like suite, evolving from metaluminous tonalites to slightly peraluminous trondhjemites (Seixas et al., 2012). Its origin is related to partial melting of a short-lived tholeiitic basaltic source rock (greenstone belt) within the hornblende-eclogite stability field in an intra-oceanic setting. This origin is supported by $\epsilon_{\text{Nd}}(t)$ values between $+2.1$ and $+1.0$ and partial melt REE modelling (Seixas et al., 2012). To the west of the Lagoa Dourada Suite, a juvenile metatonalite (Resende Costa Orthogneiss) was dated by Teixeira et al. (2015) at 2351 ± 48 Ma, yielded $\epsilon_{\text{Nd}}(t)$ mostly between $+1.1$ and $+3.2$ and $\epsilon_{\text{Hf}}(t)$ divided between depleted mantle (up to $+4.2$) and reworked zircon grains (-2.9 to -9.2). Teixeira et al. (2015), using geochemical and isotopic constraints, grouped both bodies into a geotectonic unit named the Resende Costa – Lagoa Dourada magmatic arc. The oldest reported age of plutonic rocks in the Mineiro Belt is from the Cassiterita orthogneiss (2472 ± 11 Ma to 2414 ± 29 Ma), located to the south of the Lagoa Dourada Suite. Geochemical and isotopic analyses indicate a TTG-affinity with positive $\epsilon_{\text{Nd}}(t)$ values ($+2.7$ to $+1.5$) and low $(^{87}\text{Sr}/^{86}\text{Sr})_i$ (0.700 – 0.702) (Barbosa, 2015). The Cassiterita batholith was incorporated by Barbosa et al. (2018) as part of the juvenile magmatic arc that comprises the Lagoa Dourada and the Resende Costa suites, suggesting therefore a

Table 1
Simplified isotopic-geochemical characteristics of plutonic arcs of the Mineiro Belt.

OP	Age (Ga)	Geochemistry	Isotopic constraint	T_{DM} (Ga)	Reference
1	2.47–2.41	TTG affinity, peraluminous, high Al_2O_3	$\epsilon_{Nd}(t)_{(wr)} = +2.0$	2.5 _(wr)	[1]
2	2.35	TTG affinity, metaluminous to slightly peraluminous, high Al_2O_3	$\epsilon_{Nd}(t)_{(wr)} = +1.0$ to $+2.1$;	2.4–2.5 _(wr)	[3]
2*	2.35–2.32	TTG affinity, peraluminous, high- Al_2O_3	$\epsilon_{Nd}(t)_{(wr)} = +1.1$ to $+3.2$;	2.4–2.5 _(wr)	[4]
			$\epsilon_{Hf}(t)_{(zr)} = +4.3$ to -9.0	2.3–3.4 _(zr)	
3	2.23–2.20	Sub-alkaline to calc-alkaline, metaluminous to peraluminous	$\epsilon_{Nd}(t)_{(wr)} = -0.8$ to $+2.3$	2.3–2.6 _(wr)	[5]; [6]
4	2.18–2.09	Calc-alkaline, metaluminous to peraluminous	$\epsilon_{Nd}(t)_{(wr)} = -0.2$ to -7.3	2.3–3.0 _(wr)	[2]; [7] ^a
			$\epsilon_{Hf}(t)_{(zr)} = +4.1$ to -7.0		
4**	2.13	Sanukitoid affinity high- Al_2O_3 , metaluminous	$\epsilon_{Nd}(t)_{(wr)} = +0.9$ to -1.0	2.3–2.4 _(wr)	[7] ^b ; [8]

(OP): Orogenic period; (wr): whole rock; (zr): in situ zircon.

*Resende Costa is here separated from the Lagoa Dourada Suite, but the two were grouped by Teixeira et al. (2015) (see Discussion for explanation); **Alto Maranhão has a different signature to this segment as it contains a sanukitoid affinity and abundant commingled mafic magmatic enclaves. [1] Barbosa (2015) – Cassiterita; [2] Barbosa et al. (2015) – Represa de Carmargos, Rio Grande, Macuco de Minas, Lavras-Poço de Pedra, Morro do Resende, Ribeirão do Amaral and Nazareno tonalites; [3] Seixas et al. (2012) – Lagoa Dourada tonalite; [4] Teixeira et al. (2015) – Resende Costa Suite; [5] Ávila et al. (2010); [6] Ávila et al. (2014); [7] Noce et al. (2000) –^aRitápolis, ^bAlto Maranhão; [8] Seixas et al. (2013).

protracted evolution for the oldest orogenic event in the Mineiro Belt.

The Tiradentes and Serrinha suites together with the Nazareno orthogneiss (2.26–2.21 Ga) are composed of metagranitoids with mainly granodioritic and minor tonalitic and mafic andesitic compositions. Geochemistry of the trondhjemites ranges from meta- to peraluminous, alkali-rich and low Al_2O_3 (Ávila et al., 2010, 2014). The rocks are grouped with the Serrinha-Tiradentes magmatic arc (Ávila et al., 2014). Their source was juvenile with short crustal residence, attested by $\epsilon_{Nd}(t)$ values between -0.9 and $+2.3$ and T_{DM} ages between 2.6 Ga and 2.3 Ga (Ávila et al., 2014).

The Alto Maranhão Suite is located to the south of the Congonhas Lineament, bordering the Archaean nucleus of the SSFC and is mainly composed of biotite hornblende tonalites with abundant commingled dioritic enclaves. The suite is cut by granitoids and pegmatites. The crystallization age of this suite is 2130 ± 2 Ma and its $\epsilon_{Nd}(t)$ whole rock composition is zero on average (Seixas et al., 2013). The suite resulted from the melting of the mantle wedge below a Palaeoproterozoic arc, which was previously metasomatised by TTG-like melts, similar to the model for sanukitoid genesis (Martin et al., 2010). The T_{DM} extraction line of this suite superimposes the $\epsilon_{Nd}(t)$ field of the Lagoa Dourada Suite and, thus, not only marks a change from an intra-oceanic setting (Lagoa Dourada Suite) to a continental arc setting, but is consistent with a genetic link between their sources (Seixas et al., 2013).

Other magmatic batholiths and smaller occurrences have similar ages to the Alto Maranhão Suite (ca. 2.18–2.09 Ga), have $\epsilon_{Nd}(t)$ from -0.2 to -7.3 ; $\epsilon_{Hf}(t)$ from $+4.3$ to -7.0 and are widespread in the Mineiro Belt (e.g. Ritápolis, Macuco de Minas, Serra do Camapuã, Represa de Camargos, Morro do Resende, Nazareno, Rio Grande – Seixas et al., 2013; Barbosa et al., 2015; Alkmim and Teixeira, 2017 and references therein).

4. Field relationships, sampling and methodology

Widely distributed granitoids in the Mineiro Belt are weakly to strongly-foliated, representing variable degrees of deformation and containing igneous textures. The prefix ‘meta’ is omitted in the following text as the deformation and metamorphism are not the main focus of the present study. Mafic magmatic enclaves can be either absent or abundant in some outcrops. Where they occur, they are commonly ellipsoidal with cusped margins. Macroscopically, the granitoids are biotite-rich tonalites/granodiorites with variable hornblende contents. Rock-forming minerals in the tonalites are plagioclase, quartz, biotite, amphibole, and absent to minor K-feldspar (<5 vol%). Magnetite, ilmenite, zircon, apatite, titanite, epidote and allanite are the accessory phases. Syn- to post-magmatic aplite veins crosscut the tonalites.

Twenty-two samples were collected from the main plutonic bodies. The study area is delimited by coordinates $21^\circ S$ and $20^\circ 30' S$, and $44^\circ 15' W$ to $43^\circ 30' W$ (Fig. 1c). Samples were analysed for major and trace elements at the University of Portsmouth (UK), CRPG (Nancy, France), ACME and ACT-LABS (both in Canada) laboratories. Major element compositions were analysed by X-ray Fluorescence Spectrometry (XRF) on glass beads. Trace element compositions were acquired from fragments of the same beads or from pressed powder pellets. Fifteen samples had zircon and titanite grains extracted to obtain U-Pb ages. Whole rock Sm-Nd isotope analyses were performed on eight samples at GEO-TOP-UQAM, Montreal, Canada ($n = 6$) and at the Brasília University Geochronology laboratory ($n = 2$) using the methodology described by Seixas et al. (2012, 2013). In situ zircon Lu-Hf analyses were performed on three selected samples at the University of Ouro Preto, Brazil using the methodology of Albert et al. (2016), Moreira et al. (2016) and Martínez Dopico et al. (2017). Sample LD5 is the same as Seixas et al. (2012) and had zircons analysed for U-Pb and Lu-Hf isotopes. A list of the samples used for this study and the methodology applied to each one is presented in Table 2. Detailed description of individual rock samples and localities as well as a full report on the analytical techniques is provided in Supplementary material A.

5. Results

5.1. U-Pb geochronology

Results from a U-Pb dataset of fifteen samples from the Mineiro Belt enabled the identification of magmatic episodes at ca. 2.35 Ga, ca. 2.20 Ga and ca. 2.13 Ga and one ubiquitous metamorphic event at ca. 2.050 Ga, after investigation of the zircon and titanite morphology and internal structures. A summary of the ages is presented in Table 3. In this section, the new analyses for samples 14-SCT-01, 16-RC-01 and 16-RC-03 are presented. Description of other samples are available in Supplementary material A, and analytical data are presented in Supplementary material C.

Zircons from sample 14-SCT-01 are transparent to pale white, elongated and prismatic with fine oscillatory zoning (Fig. 3a). Apatite inclusions are common. Forty-nine analyses were carried out on thirty-five grains. Five analyses, including three cores, yielded Archaean ages between 2660 Ma and 2970 Ma, whereas the other analyses are Rhyacian. Twenty-six analyses yield an upper intercept age of 2122 ± 3.5 Ma (Fig. 4a). Few grains are concordant to sub-concordant between 2100 Ma and 2020 Ma (Fig. 4c). The same sample also had five zircons analysed via ID-TIMS and four yielded a best fit line with upper intercept age of 2121 ± 2 Ma (Fig. 4b). Titanite grains from the same sample are sub-angular and

Table 2
Summary of methodology applied to each sample of this study. See Fig. 1c for sampling localities.

Sample	Plutons/suites	Geochemistry - Major and trace elements	U-Pb zircon (z); titanite (t)	Whole rock Sm-Nd	In situ zircon Lu-Hf
LD5	Lagoa Dourada		X _(z)		x
14-LDT-01		x	X _(z)		
16-LD-4A		x	X _(z)		
16-RC-1A	Resende Costa	x	X _{(z);(t)}		
16-RC-3A		x	X _(z)		
17-2130	Bombaça		X _(z)		x
17-BÇ47		x		x	
17-GAGE-1	Gagé	x		x	
17-GAGE-2		x		x	
14-AMT-01a	Alto Maranhão	x			
14-AMT-01b		x			
14-AMT-02		x	X _(z)		
14-AMT-03		x	X _{(z);(t)}		
14-SCT-01	Serra do Camapuã	x	X _{(z);(t)}	x	x
17-SC713		x			
17-SC3		x		x	
17-SC4		x			
16-SBS-1A	São Brás do Suaçuí	x	X _{(z);(t)}	x	
16-SBS-1C		x	X _(z)		
16-SBS-2B		x	X _{(z);(t)}	x	
16-MS-1D	Água Limpa	x	X _(z)	x	
16-CGT-01	Casa Grande	x	X _(z)		
16-CGT-03		x	X _(z)		

honey brown in colour (Fig. 3a). Twenty-two grains were analysed and fourteen yielded a concordia age of 2136 ± 7 Ma (Fig. 4b). One grain returned a $^{207}\text{Pb}/^{206}\text{Pb}$ age of 2064 ± 28 Ma which is 100% concordant. The other seven analyses are slightly discordant.

Zircon grains from samples 16-RC-1A and 16-RC-3A are sub-hedral to euhedral, and short prismatic. The most evident feature of the grains in CL is a core-rim structure. Most (90%) grains show

bright cores surrounded by homogeneous dark rims (Fig. 3b). Cores contain fine oscillatory zoning, whereas rims are homogeneous. A few grains show indentation between core and rim. One hundred and twenty U-Pb zircon analyses (70 cores, 50 rims) were acquired from both samples. They yielded similar results and therefore are plotted together in a concordia diagram (Fig. 4d). Cores return ages around 2350 Ma (upper intercept age at 2352 ± 11 Ma) while the

Table 3
Summary of ages by this study for plutonic rocks in the Mineiro Belt.

Sample	Inherited age (Ma)	Zircon crystallisation age (Ma)	Zircon metamorphic age (Ma)	Titanite crystallisation age (Ma)	Titanite metamorphic age (Ma)
LD5		$2356 \pm 4_{(\text{conc})}$			
14-LDT-01		$2347 \pm 7_{(\text{int})}$			
16-LD-4A		$2345 \pm 12_{(\text{int})}$			
16-RC-1A	$2358 \pm 38_{(\text{int})}$	$2122 \pm 84_{(\text{int})}$		$2148 \pm 6_{(\text{conc})}$	$2086 \pm 33_{(\text{ind} - 2\%)}$
16-RC-3A	$2365 \pm 36_{(\text{int})}$	$2149 \pm 74_{(\text{int})}$			
16-RC ^a	$2358 \pm 38_{(\text{int})}$	$2151 \pm 31_{(\text{int})}$			
14-AMT-02		$2149 \pm 30_{(\text{int})}$		$2135 \pm 9_{(\text{conc})}$	$2059 \pm 31_{(\text{ind}-2\%)}$
14-AMT-03		$2135 \pm 12_{(\text{int})}$		$2122 \pm 7_{(\text{conc})}$	$2045 \pm 31_{(\text{ind}-2\%)}$
17-2130		$2118 \pm 7_{(\text{int})}$			
14-SCT-01	$>2670 \pm 18$	$2137 \pm 80_{(\text{int})}$	$2031 \pm 17_{(\text{ind}-6\%)}$	$2136 \pm 7_{(\text{conc})}$	$2064 \pm 28_{(\text{ind}-0.5\%)}$
		$2121 \pm 2_{(\text{int})}$ (TIMS)	$2068 \pm 25_{(\text{ind}-0\%)}$		
		$2123 \pm 4_{(\text{int})}$	$2057 \pm 19_{(\text{ind}-0.2\%)}$		
16-SBS-1A		$2127 \pm 25_{(\text{int})}$	$2062 \pm 30_{(\text{ind}-1\%)}$	$2136 \pm 14_{(\text{conc})}$	$2054 \pm 17_{(\text{ind}-2\%)}$
		$2121 \pm 42_{(\text{ind}-1\%)}$			
16-SBS-1C	$>2333 \pm 34_{(\text{ind}-2\%)}$	$2122 \pm 8_{(\text{conc})}$	$2082 \pm 24_{(\text{ind}-5\%)}$		
		$2121 \pm 24_{(\text{ind}-0\%)}$	$2023 \pm 16_{(\text{ind}-4\%)}$		
16-SBS-2B	$>2251 \pm 56_{(\text{ind}-4\%)}$	$2136 \pm 9.6_{(\text{conc})}$	$2018 \pm 33_{(\text{ind}-3\%)}$		
16-MS-1D		$2186 \pm 11_{(\text{conc})}$			
		$2173 \pm 18_{(\text{int})}$			
16-CGT-01		$2149 \pm 4.3_{(\text{conc})}$			
16-CGT-03		$2167 \pm 14_{(\text{conc})}$			
		$2200 \pm 20_{(\text{int})}$			

(conc): U-Pb concordia age; (int): U-Pb intercept age; (ind-n%): $^{207}\text{Pb}/^{206}\text{Pb}$ individual age – discordance percentage.

^a Two samples of the Resende Costa Suite plotted together.

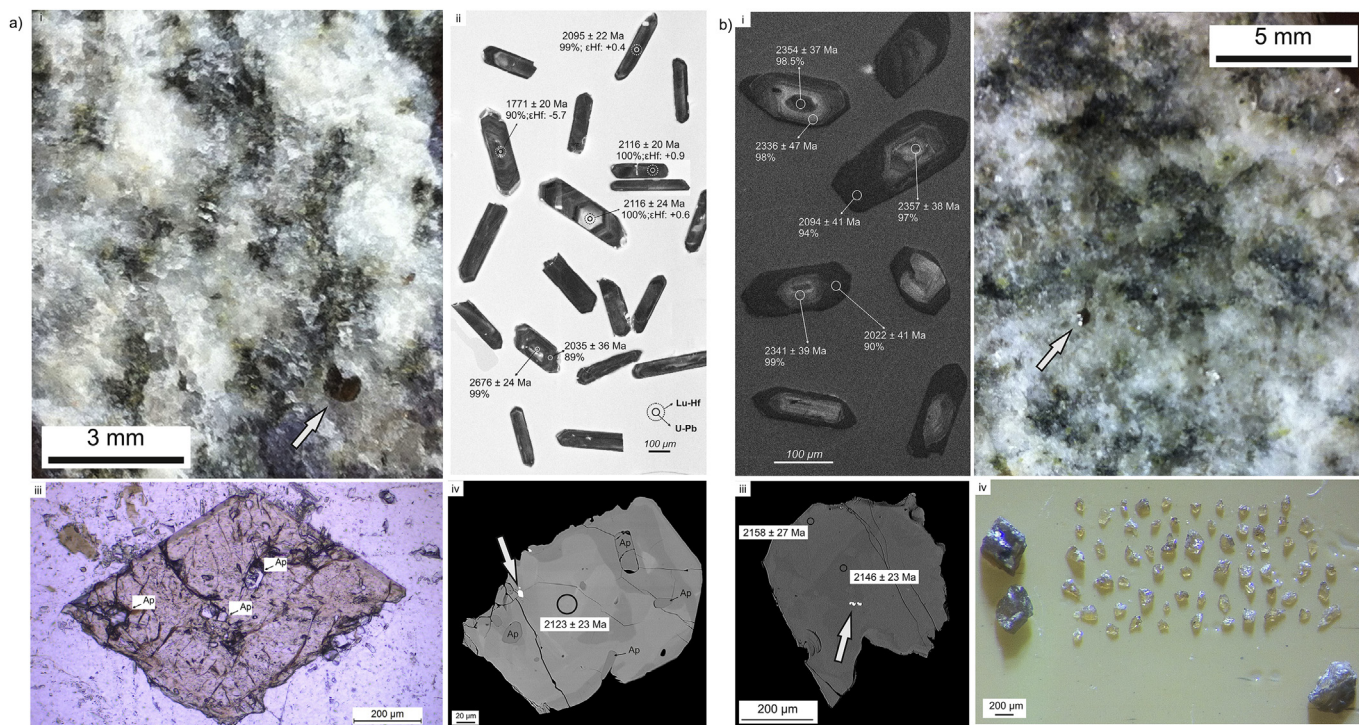


Figure 3. (a) Zircons and titanites from sample 14-SCT-01: (i) millimetre-size titanite grain indicated by white arrow in hand size sample; (ii) CL image, $^{206}\text{Pb}/^{238}\text{U}$ ages and degree of concordance of zircons. Available Lu-Hf spot analyses shown; (iii) plane polarised light microscope image of euhedral titanite. Apatite inclusions (Ap) indicated; (iv) BSE image of titanite containing apatite and zircon inclusions. $^{206}\text{Pb}/^{238}\text{U}$ age of 2123 ± 23 Ma from the core. (b) Zircons and titanites from Resende Costa Suite samples: (i) CL image of zircons from sample 16-RC-3A. $^{207}\text{Pb}/^{206}\text{Pb}$ ages indicated; (ii) millimetre size titanite of sample 16-RC-1A indicated by white arrow; (iii) BSE image of dated titanite (light and dark domains yielded same $^{206}\text{Pb}/^{238}\text{U}$ age within uncertainty); (iv) hand-picked titanite fragments/grains of sample 16-RC-1A used for U-Pb analyses. Zircon inclusions indicated by white arrow.

rims are significantly younger at around 2130 Ma (upper intercept age at 2151 ± 31 Ma). Core analyses define a strong Pb-loss trend, with a lower intercept at around 500 Ma. Titanite grains from this suite are euhedral, yellow honey to brown in colour and abundant in both samples, reaching 500 μm in size (Fig. 3b). Titanite grains show igneous texture in BSE imaging, distinguished by patchy zoning patterns and local overgrowths, commonly possessing zircon inclusions up to 15 μm (Fig. 3b). Noteworthy and contrary to examples from the literature (Storey et al., 2006; Khon, 2017), Pb in the titanite grains from sample 16-RC-1A is all radiogenic within uncertainty and detection limits (Fig. 4e), therefore no common Pb correction was applied. Analyses are concordant (>97%), except for one analyses that was not considered for age calculation. Fourteen analyses give a consistent concordia age of 2148 ± 6 Ma. Zircon rims and titanite ages overlap within uncertainty (Fig. 4f).

U-Pb zircon and titanite ages in this work are in good agreement with previously published zircon and titanite U-Pb ages from the Mineiro Belt (Noce et al., 2000; Seixas et al., 2012, 2013; Barbosa et al., 2015; Teixeira et al., 2015; Aguilar Gil et al., 2017). Titanite grains have two distinct groups of ages, at around 2130 Ma and a less abundant one around 2050 Ma. Overall, zircon and titanite ages of tonalites (17-2130; 16-SBS-1A; 16-SBS-1C and 16-SBS-2B) and the Serra do Camapuã Pluton (14-SCT-01) overlap with the Alto Maranhão Suite, consistent with a genetic link between them. Sample 16-MS-1D is significantly older than Alto Maranhão samples (by 40–50 Ma). An older as yet unidentified crustal contribution should be present in the region, judging by the xenoliths and the few Archaean inherited zircons in samples 16-SBS-1C and 14-SCT-01. Archaean Hf and Nd model ages also indicate older crustal materials inherited from the surrounding terranes (Seixas et al., 2012; Barbosa et al., 2015; Teixeira et al., 2015).

5.2. Geochemistry

Major, trace and REE elements for all samples are presented in [Supplementary material B](#). Geochemistry of most granitoids is consistent with the TTG field defined by [Moyen and Martin \(2012\)](#) and verified by the normative feldspar classification diagram (Ab-An-Or ternary feldspar diagram of [O'Connor, 1965](#); with the granitoid fields defined by [Barker, 1979](#)) (Fig. 5a), the La/Yb fractionation diagram (Fig. 5b) and the Sr and Y contents (Fig. 5c). The normalised La/Yb vs. Yb diagram divides the samples into two groups: Lagoa Dourada Suite plus Resende Costa trondhjemitic and remaining samples with higher La/Yb ratio and Yb concentration (the highest being samples 17-BÇ47 and 14-AMT-03, Fig. 5b). Similarly, lower (La/Yb)_n samples have lower Y concentration. In the diagram by [Condie \(2005\)](#) (see also [Smithies, 2000](#), [Smithies et al., 2009](#)), Lagoa Dourada and Resende Costa suites (low La/Yb) show relative depletion of Mg# against SiO₂ and lie in the TTG field. Samples from the Alto Maranhão Suite have high (La/Yb)_n and lie in the adakite field (Fig. 5d). In general, calc-alkaline samples are metaluminous to slightly peraluminous (i.e. A/CNK ≤ 1.03 , except for the two Resende Costa samples with A/CNK of 1.13–1.15). Their chondrite-normalized REE patterns indicate enrichment in LREE relative to HREE, flat to steep HREEs and negligible or small positive Eu anomalies (Fig. 6). Ba + Sr increase in younger samples, accompanied by higher (La/Yb)_n (Fig. 7a). The Sr/Ba isolines diagram shows that samples that have ratios between 0.5 and 1.5 (Fig. 7b), have high Ba-Sr content up to 2000 ppm (Fig. 7a, c). The exception is the Lagoa Dourada Suite with ratios up to 5.0 and Ba + Sr up to 700 ppm.

Most samples plot in the high-HREE TTG field of [Halla et al. \(2009\)](#), whereas only samples from the Alto Maranhão Suite are

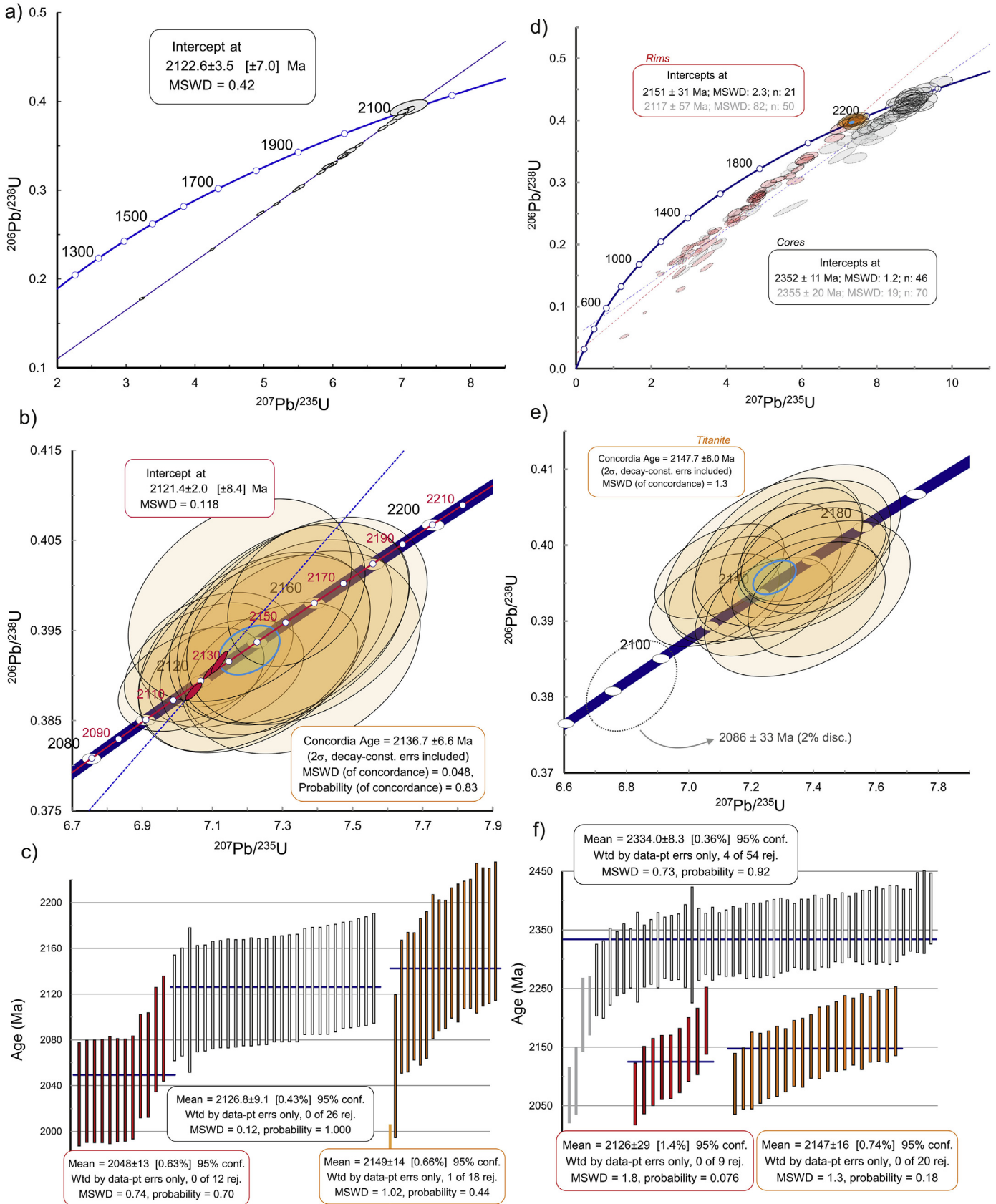


Figure 4. U-Pb analyses of samples 14-SCT-01, 16-RC-1A and 16-RC-3A. (a) LA-ICP-MS analyses of zircons from sample 14-SCT-01. (b) Zircon ID-TIMS analyses and titanite LA-ICP-MS analyses from sample 14-SCT-01. Titanite analyses are within uncertainty of zircon intercept age (2121 ± 2 Ma), although yielding an older concordia age (ca. 2136 Ma). (c) Weighted mean average of zircon and titanite $^{207}\text{Pb}/^{206}\text{Pb}$ ages obtained from sample 14-SCT-01 displayed with propagated 2σ uncertainties and 2% added in quadrature to account for systematic uncertainty (see Horstwood et al., 2016; Spencer et al., 2016). Red and white bars correspond to zircon ages and orange bars correspond to titanite ages. Zircon and

in the sanukitoid field (Fig. 7d). A trace element mantle-normalised diagram shows Nb-Ta, Ti negative anomalies, and positive Sr anomalies (Fig. 6).

Three different geochemical groups can be distinguished for plutonic rocks in the Mineiro Belt: (1) TTGs with low Mg#, (La/Yb)_n, Ba+Sr and (Gd/Er)_n content; (2) sanukitoids with high Mg#, (La/Yb)_n, Ba+Sr, (Gd/Er)_n; and (3) hybrid granitoids, akin to the second group but depleted in compatible elements (Fig. 4). The third group seems to fit the geochemical interval between the first and second in the ternary diagram of Laurent et al. (2014). Compared to the gneisses and granitoids studied by Farina et al. (2015) and Moreno et al. (2017) (see the Geological Background and Rationale above), the presence of high Ba-Sr magmas and lack of two-mica granites in the Mineiro Belt plutons differs from the basement rocks of the SSFC (Fig. 8). A₂-type granitoids from Moreno et al. (2017) mostly plot in the fields corresponding to hybrid and biotite, two-mica granites of Laurent et al. (2014) (Fig. 8).

The Lagoa Dourada Suite (14-LDT-01 and 16-LD-4A) and Resende Costa Suite (16-RC-1A and 16-RC-3A) have generally negative slopes between the large ion lithophile (LIL) and the high-field-strength (HFS) elements with negative anomalies for Nb-Ta and Ti (Fig. 6). These suites have lower trace element contents than other surrounding granitoids in the Mineiro Belt. However, samples from the Lagoa Dourada Suite have relatively flat patterns of LIL elements, particularly K, Rb, Ba, and Pb and higher Mg and Fe contents compared to the Resende Costa trondhjemites, which suggests more fractionation and differentiation of the trondhjemites. On the other hand, Resende Costa trondhjemite samples are more depleted in HFS elements and REE than the Lagoa Dourada rocks. These two suites of the Mineiro Belt fit well within the TTG field following the classification of Laurent et al. (2014) and could be described as low-HREE TTGs (Moyen and Martin, 2012) (Fig. 5d). Geochemical data from the Cassiterita orthogneiss (Barbosa, 2015) show similar trends to the Lagoa Dourada and Resende Costa suites, although the LREE are slightly enriched (not shown).

A main difference between samples from the Alto Maranhão Suite (14-AMT-01a, b; 14-AMT-02 and 14-AMT-03) and the Lagoa Dourada and Resende Costa samples, besides enrichment in compatible elements (e.g. Cr, Mg, Ni), is the enrichment of LIL elements, principally Ba and Sr. A similarity of these rocks is the general negative correlation between light and heavy REE and in the mantle-normalized trace element pattern (Fig. 6). This duality of mantle and crustal signature is typical of sanukitoids (Fig. 8); this suite was accordingly described as low-Ti sanukitoid by Seixas et al. (2013). The Alto Maranhão Suite is more depleted in the HREE and in some HFS elements, such as Nb and Zr, compared to the average composition of sanukitoids from the Limpopo Belt and Pietersburg block in South Africa. In addition, the Alto Maranhão Suite has no monzogranitoids with feldspar phenocrysts, which are common in Archaean sanukitoids.

Several ca. 2.13 Ga tonalite bodies (São Brás do Suaçuí – 16-SBS-1A, 16-SBS-1C and 16-SBS-2B; Bombaça – 17-BÇ47, 17-2130; Gagé – 17-GAGE-1, 17-GAGE-2) are peraluminous to metaluminous, calc-alkaline and richer in K₂O compared to samples from the Resende Costa and Lagoa Dourada suites. REE patterns are similar to the biotite- and two-mica granites (Fig. 6) and they can be classified as hybrid granitoids (Laurent et al., 2014) (Fig. 8). Sample 16-MS-1D is less evolved. Firstly, the sample is relatively depleted in REE and

has a positive Eu anomaly. Secondly, this sample is more Ca-enriched, metaluminous and relatively depleted in LREE, although in the McDonough and Sun (1995) mantle-normalised diagrams the samples do not show a striking difference. Samples from Serra do Camapuã Pluton (14-SCT-01; 17-SC713; 17-SC3 and 17-SC4) are metaluminous to peraluminous trondhjemite-granodiorite and have enrichment of LREE relative to HREE. Samples have positive to slightly negative Eu anomalies and, as shown in the McDonough and Sun and (1995) spider diagram, have similar patterns to the biotite- and two-mica granitoids (Fig. 6). Samples plot in the area corresponding to the overlap between hybrid granitoid and TTG fields (Fig. 8).

Samples 14-CGT-01 and 14-CGT-03 from the Casa Grande tonalite are described separately due to their different mafic composition. Sample 14-CGT-03 plots in the gabbroic field of the TAS diagram of Cox et al. (1979) (not shown). This sample was collected from a mafic portion of the tonalite (see sample description in the Supplementary file) and is composed of 40%–50% mafic minerals (hornblende + biotite + magnetite). This segregated portion of the outcrop also plots in the field of the mafic magmatic enclaves of the Alto Maranhão Suite in the AFM diagram. Among other possibilities, this segment of the tonalite represents an incompletely-mixed enclave. This sample is also enriched in HREE compared to other samples from this study. Sample 14-CGT-01 is also more mafic than the other tonalites and has intermediate silica content (60 wt.%), classified as a diorite. Ba and Sr contents of this sample are ca. 600 ppm each, but reach ca. 450 ppm and 400 ppm in sample 16-CGT-03. Both samples plot in the sanukitoid field in the Laurent et al. (2014) diagram, biased by their Mg# and FeO^t abundance.

5.3. Sm-Nd isotope analyses

Table 4 reports the Nd isotopic composition of eight samples from selected plutons in the Mineiro Belt. The results for all the analysed rocks are presented in an ϵ_{Nd} versus time diagram in Fig. 9a. Sample 17-2130 has Sm-Nd T_{DM} age of 2.4 Ga and yields $\epsilon_{Nd}(t)$ value of -1.0 for a crystallisation age of 2130 Ma. Sample 14-SCT-01, from the Serra do Camapuã Pluton, yields $\epsilon_{Nd}(t) = -0.8$ at 2121 Ma, with Sm-Nd T_{DM} age of ca. 2.5 Ga. Another sample (17-SC3) collected from the same quarry yields similar values within uncertainty, confirming the homogeneous isotopic character of the pluton. Samples 17-GAGE-1 and 17-GAGE-2 yield respectively $\epsilon_{Nd}(t)$ of -0.1 and 0.1 and both have Nd T_{DM} ages of 2.4 Ga for an estimated age of 2130 Ma. Sample 16-SBS-1A has a model age of 2.3 Ga and $\epsilon_{Nd}(t) = +0.3$ at 2130 Ma. Sm-Nd isotopes suggest a mantle-derived source, but crustal contribution is assumed during their genesis considering the presence of some Archaean inherited zircons in the spatially and temporally correlated sample 16-SBS-1C. Data from sample 16-SBS-2B yield $T_{DM} = 2.4$ Ga, $\epsilon_{Nd}(t) = -0.2$ at 2130 Ma. Sample 16-MS-1D has T_{DM} age of 2.6 Ga and $\epsilon_{Nd}(t) = -2.9$ at 2180 Ma.

Samples have $\epsilon_{Nd}(t)$ close to zero and crystallisation ages at around 2130 Ma, except for sample 16-MS-1D, which is ca. 50 Ma older than the other rocks analysed for Sm-Nd isotopes. These two features are found in the Alto Maranhão Suite (Seixas et al., 2012). The Nd T_{DM} ages range from 2.3 Ga to 2.4 Ga, apart from the Serra do Camapuã (14-SCT-01 and 17-SC3) and 16-MS-1D samples, which have model ages of 2.5 Ga and 2.6 Ga.

titanite ages overlap within uncertainty (d) U-Pb zircon analyses of samples 16-RC-1A and 16-RC-3A. Red and grey ellipses represent zircon rim and core analyses, respectively. They yielded different intercept ages at ca. 2120 Ma (rim) and ca. 2350 Ma (core). U-Pb titanite analyses from sample 16-RC-1A are plotted in the same diagram and return ages within uncertainty of the zircon rims. (e) Concordia age of U-Pb titanite analyses in detail. One analysis at ca. 2086 Ma was not used for the concordia age calculation. (f) Weighted mean average of zircon and titanite $^{207}\text{Pb}/^{206}\text{Pb}$ ages obtained from samples 16-RC-1A and 16-RC-3A displayed as (c). White and red bars correspond to zircon core and rim analyses, respectively. Orange bars represent titanite ages.

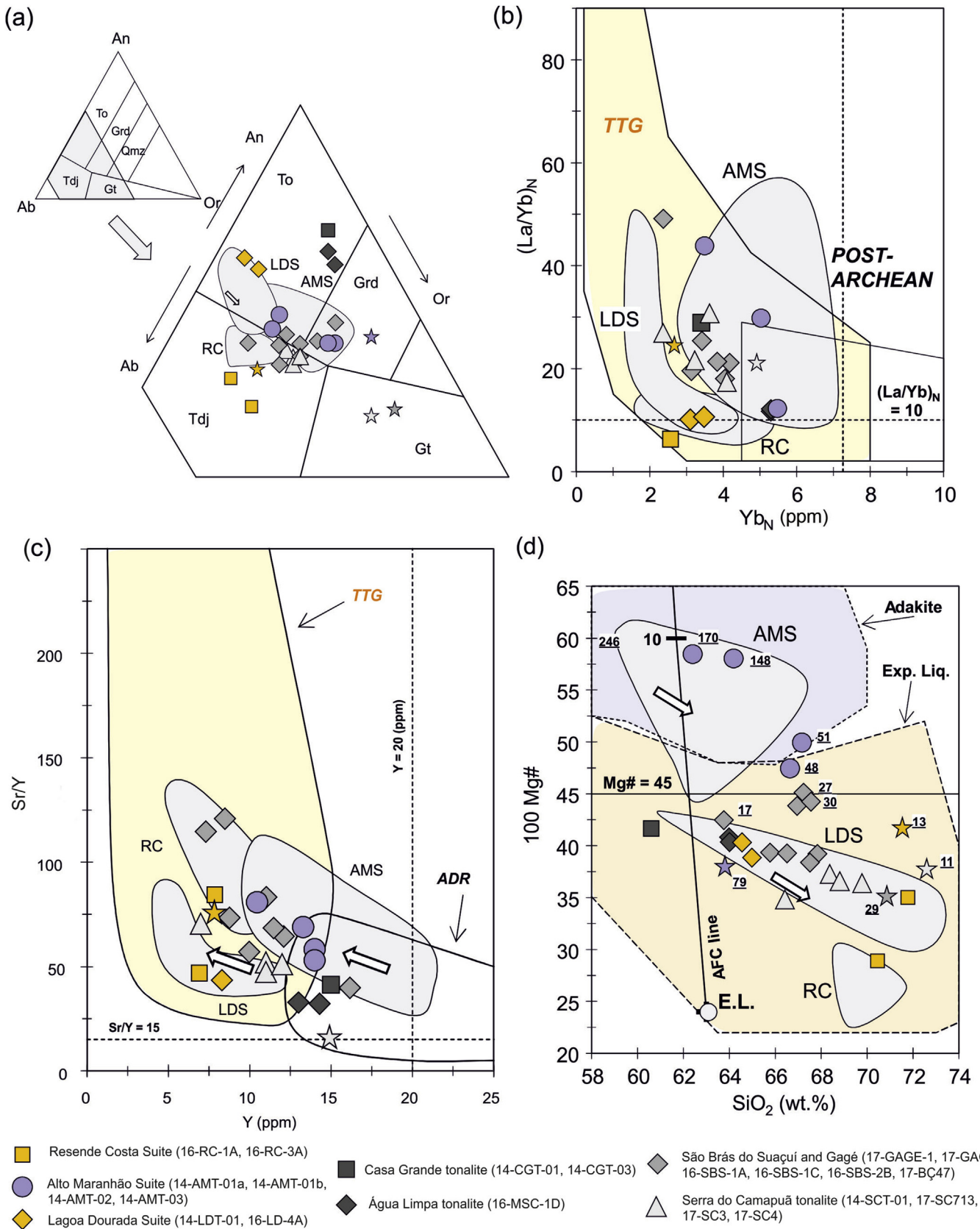


Figure 5. Classification diagrams of the studied granitoids. Also plotted: Palaeoproterozoic LDS – Lagoa Dourada Suite (Seixas et al., 2012), AMS – Alto Maranhão Suite (Seixas et al., 2013) and RC – Resende Costa Suite (Teixeira et al., 2015); and representative Neoproterozoic granitoids (according to Laurent et al., 2014). Symbols for the average composition of high aluminium TTG suites (TTG – yellow star), mantle derived sanukitoid suites (SK – purple star), hybrid granitoids (HYB – grey star), and crustal derived granitic suites (GT – white star). For the LDS and AMS, parental to evolved magma compositions are indicated by an arrow, and the field shows the spread of the compositions of each suite. (a) Normative An-

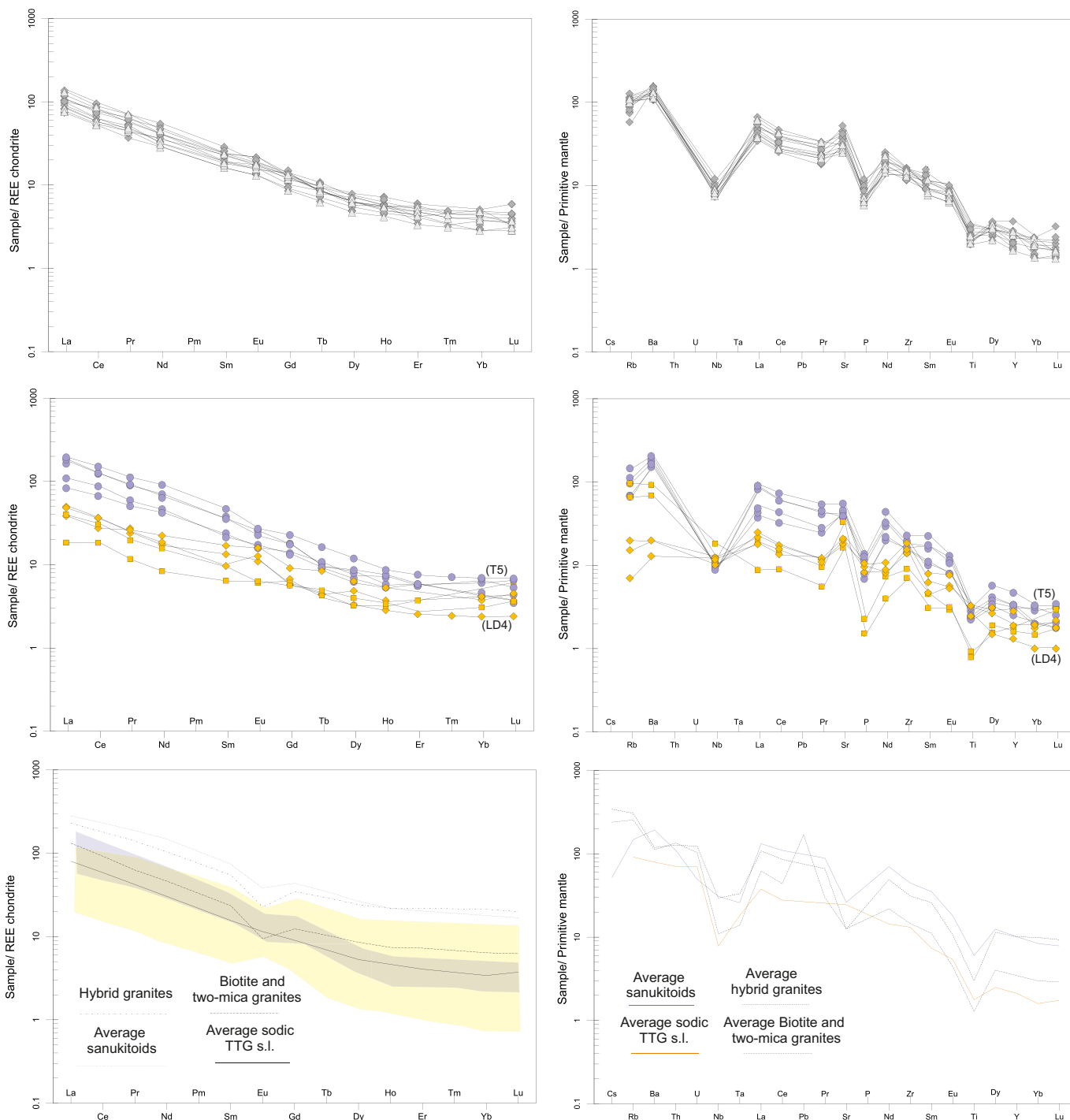


Figure 6. Left column: Average chondrite-normalized REE patterns for studied samples. Yellow field of TTGs and purple field of sanukitoids are drawn using the compositions of high and low-pressure TTGs and medium-HREE sanukitoid group (Halla et al., 2009). Normalization values are from Boynton (1984); Right column: Mantle-normalized multi-element plots (McDonough and Sun, 1995). Average sodic TTG composition from Moyen and Martin (2012); average sanukitoid; biotite, two-mica and hybrid granitoids compositions from Laurent et al. (2014). Legend as Fig. 5. Samples LD4 and T5 from Seixas et al. (2012, 2013) are also plotted in the middle and bottom diagrams as indicated. Samples 14-CGT-01 and 14-CGT-03 are not plotted.

Ab-Or triangle (O'Connor, 1965), with subdivisions modified by Barker (1979). Tdj = trondhjemite, To = tonalite, Grd = granodiorite, Gt = granite, Qmz = quartz monzonite. Sample 14-CGT-03 (<10% normative Qz) is not in this diagram. The field for Archean TTGs is from Moyen and Martin (2012); (b) The $(La/Yb)_n$ vs. Yb_n diagram, with the field for Archean high-aluminium TTG suites and post-Archean granitoids according to Martin (1986). (c) Sr/Y vs. Y diagram, field of Archean high-aluminium TTG suites and ADR (calc-alkaline post-Archean Andesite-Dacite-Rhyolite suites) from Drummond and Defant (1990). (d) Mg# against silica content for the studied granitoids. Adapted from Condie (2005), with the delimitation of the compositional field of adakitic volcanic rocks and experimental melts derived from metabasalt. AFC = assimilation fractional crystallization model for the pathway of a metabasalt-derived experimental liquid (E.L.) through the mantle wedge, tick line = 10% AFC. Underlined numbers show chromium content in ppm of selected samples. Sample 14-CGT-03 (51 wt.% SiO₂) is not in this diagram. SK and HYB granitoid averages are not represented in (b) and (c) diagrams because of higher contents in Yb_n and Y, respectively.

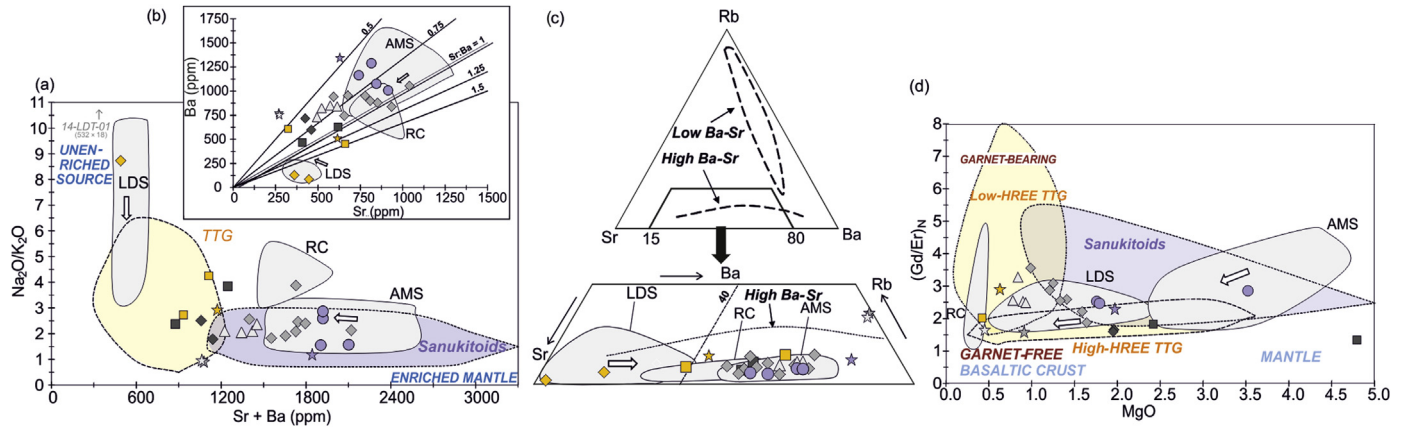


Figure 7. (a) Classification of the studied granitoids in the Sr + Ba vs. $\text{Na}_2\text{O}/\text{K}_2\text{O}$ diagram proposed by Halla et al. (2009). Inset (b) shows the content of Sr and Ba and the lines for equal Sr/Ba ratio. Legend as Fig. 5. Triangular diagram Rb–Ba–Sr (c), with the field for Low and High Ba–Sr granites from Tarney and Jones (1994). (d) $(\text{Gd}/\text{Er})_n$ vs. MgO diagram (Halla et al., 2009). Legend as Fig. 5.

5.4. Lu–Hf isotope analyses

Fifty-eight Lu–Hf analyses were performed on top of U–Pb analyses on zircons from samples LD5, 17-2130 and 14-SCT-01 (Fig. 9b). Hf analyses on zircons from the Lagoa Dourada sample (LD5 – concordia U–Pb age of 2356 ± 4 Ma) plot in a narrow field with $\epsilon_{\text{Hf}}(2350\text{Ma})$ values between +4.3 and +5.6, consistent with a juvenile origin. One grain had core and rim analysed and yielded similar $^{207}\text{Pb}/^{206}\text{Pb}$ age and $\epsilon_{\text{Hf}}(t)$ within uncertainty, respectively of 2356 ± 22 Ma, 4.3 ± 0.8 (grain 34c) and 2357 ± 21 Ma, 4.9 ± 0.6 (grain 34r). Model ages range from 2.37 Ga to 2.44 Ga. Data are consistent with published Sm–Nd isotopes from the same sample ($\epsilon_{\text{Nd}}(2350\text{Ma}) = +2.1$, $\text{Nd } T_{\text{DM}} = 2.4$ Ga – Seixas et al., 2013) as well as with published data from nearby plutons (Barbosa et al., 2015; Teixeira et al., 2015). Nineteen Hf analyses were carried out on zircons from sample 17-2130. $\epsilon_{\text{Hf}}(2120\text{Ma})$ ranges from -1.2 ± 0.7

to 0.9 ± 0.8 (2σ error) with an average of zero and the Hf T_{DM} ages range from 2.44 Ga to 2.55 Ga. Results are compatible with Sm–Nd analyses of the whole rock and the near-chondritic signature attests to the juvenile origin of the magma. Nineteen Hf analyses on zircons from sample 14-SCT-01 yielded $\epsilon_{\text{Hf}}(2121\text{Ma})$ from -11.4 to $+1.4$ and respectively, Hf T_{DM} ages of 3.11–2.41 Ga. Negative values are due to a few analysed grains, which are 6%–10% discordant. The U–Pb discordance shifts the ϵ_{Hf} towards negative values even when the $\epsilon_{\text{Hf}}(t)$ is calculated at the preferred age of the grain or rock (Vervoort and Kemp, 2016). In fact, the selected 100% concordant grains only give $\epsilon_{\text{Hf}}(t)$ values at around zero, which matches the near chondritic $\epsilon_{\text{Nd}}(t)$ of the whole rock.

6. Discussion

In the following, we explore why the juvenile additions to the crust were high in the Mineiro Belt during the Palaeoproterozoic magmatic lull, the evolution of the region through successive episodes of magmatic arc amalgamation, geochemical evolution compared with that proposed for Archaean granitoids (e.g. Laurent et al., 2014) and future directions in the study of Siderian and Rhyacian plutonism.

6.1. Juvenile nature of Mineiro Belt

Most Sm–Nd and Lu–Hf analyses of granitoids in the Mineiro Belt indicate juvenile to chondritic signatures (Ávila et al., 2010, 2014; Seixas et al., 2012, 2013; Teixeira et al., 2015; this study). In general, $\epsilon_{\text{Nd}}(t)$ is around zero and the similar Nd T_{DM} implies a short-lived Palaeoproterozoic source for the parent rocks, after which they remelted to generate the existing granitoids (Table 4). The exception is sample 16-MSC-1D, which has a $\epsilon_{\text{Nd}}(2180\text{Ma})$ value of -2.9 . This negative value is derived from crustal assimilation of amphibolite rafts included within the tonalite (see Supplementary material A). The superposition of ϵ_{Nd} and depleted mantle evolution line of the amphibolite (sample TH; Seixas et al., 2012) reinforces this hypothesis. This is because the amphibolites have Nd T_{DM} of 3.3 Ga and evolve to negative ϵ_{Nd} values at the age of the tonalite crystallisation (2.18 Ga) when the assimilation most likely occurred (Fig. 9a).

The Lagoa Dourada Suite has whole rock Sm–Nd T_{DM} ages between 2400 and 2500 Ma, which implies short crustal residence time, with significant positive $\epsilon_{\text{Nd}}(2350\text{Ma})$ between +1.0 and +2.1 and $\epsilon_{\text{Hf}}(2350\text{Ma})$ up to +5.6. The Lu–Hf T_{DM} ages range between

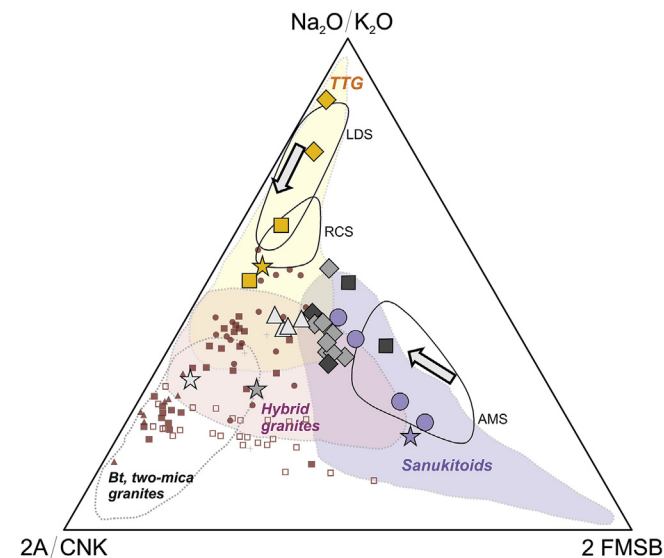


Figure 8. Archaean and Palaeoproterozoic geochemistry and isotopic data from the SSFC. Ternary classification diagram from Laurent et al. (2014). Triangle vertices are: $2 \times \text{A}/\text{CNK}$ (molar $\text{Al}_2\text{O}_3/(\text{CaO} + \text{K}_2\text{O} + \text{Na}_2\text{O})$ ratio); $\text{Na}_2\text{O}/\text{K}_2\text{O}$ and $2 \times (\text{FeO}^\dagger + \text{MgO}) \times (\text{Sr} + \text{Ba}) \text{ wt.}\%$ (=FM/SB). Red symbols are Archaean TTG and K-granitoids from Farina et al. (2015). Open red squares are from Moreno et al. (2017). Legend as Fig. 5.

Table 4
Nd isotope composition of studied samples.

Sample	Age (Ga)	Sm (ppm) ^a	Nd (ppm) ^a	¹⁴⁷ Sm/ ¹⁴⁴ Nd ^a	¹⁴³ Nd/ ¹⁴⁴ Nd ^b	2σ	ε _{Nd} (0)	ε _{Nd} (t) ^c	T _{DM} (Ga) ^d
17-GAGE-1	2.130	3.1	16.9	0.1100	0.511417	15	−23.8	−0.1	2.4
17-GAGE-2	2.130	4.4	22.0	0.1203	0.511575	10	−20.7	+0.1	2.4
17- BÇ47	2.130	5.1	30.9	0.1005	0.511241	5	−27.3	−1.0	2.4
14-SCT-01	2.121	4.0	20.8	0.1173	0.511486	7	−22.5	−0.8	2.5
17-SC3	2.121	3.6	20.0	0.1079	0.511333	9	−25.4	−1.2	2.5
16-SBS-1A	2.130	4.8	29.0	0.0991	0.511284	9	−26.4	+0.3	2.3
16-SBS-2B	2.130	3.6	20.5	0.1065	0.511367	10	−24.8	−0.1	2.4
16-MS-1D	2.180	3.0	16.9	0.1084	0.511223	11	−27.6	−2.9	2.6

^a Sm and Nd concentrations and ¹⁴⁷Sm/¹⁴⁴Nd ratios accurate within 0.5%.

^b ¹⁴³Nd/¹⁴⁴Nd normalized to ¹⁴⁶Nd/¹⁴⁴Nd = 0.7219.

^c ε_{Nd}(t) values from crystallization ages and chondritic ratios of ¹⁴³Nd/¹⁴⁴Nd = 0.512638 and ¹⁴⁷Sm/¹⁴⁴Nd = 0.1966.

^d Nd model ages calculated using depleted mantle model of DePaolo (1981). Maximum error is 0.5 ε_{Nd} units.

2370 Ma and 2440 Ma. This defines the depleted mantle source. Noticeably, Lu-Hf analyses of zircons from this suite yielded a crustal residence time as short as 15–20 Ma. The generally shorter crustal residence time of the Lagoa Dourada Suite suggests a relatively thinner and mafic crustal segment during the periods of magma emplacement (Dhuime et al., 2015).

In contrast, the Resende Costa Suite has older Hf T_{DM} ages in ca. 2350 Ma grains, ranging from 2400 Ma to 3400 Ma and one grain has ε_{Hf}(t) as low as −9.0. However, whole rock ε_{Nd}(2350Ma) between +1.1 and +3.2 and the ε_{Hf}(2350Ma) of the spatially related Restinga de Baixo amphibolite (mostly between +4 and +7) suggests a juvenile signature (Fig. 9b) (Teixeira et al., 2015).

The Serrinha-Tiradentes Suite (Ávila et al., 2010, 2014) and the Alto Maranhão Suite (Seixas et al., 2013) dated at 2.23 Ga and 2.13 Ga are juvenile segments of the Mineiro Belt, due to their ε_{Nd}(t) signatures up to +2.3 and +0.9, respectively. Roughly contemporary plutonic rocks dated between 2.17 Ga and 2.12 Ga also display positive ε_{Nd}(t) and ε_{Hf}(t) and broaden the isotopic composition, yet confer a juvenile signature to the belt (Table 1).

Volcanoclastic sequences around main plutonic bodies in the Mineiro Belt are rich in mafic volcanic rocks with juvenile isotopic signatures, consistent with an intra-oceanic setting (Ávila et al., 2010, 2014). Juvenile tonalites of the Mineiro Belt represent a shift to a ca. 2.13 Ga continental arc with mantle wedge interaction, in agreement with previous tectonic models (Seixas et al., 2013; Barbosa, 2015; Barbosa et al., 2015). The diversity of other magmatic occurrences in the Mineiro Belt corresponds to magmatic differentiation of the sanukitoid end member.

Supracrustal sequences in the Mineiro Belt contain Archaean detrital zircons but have maximum deposition ages of ca. 2100 Ma and ca. 2300 Ma, an interval of hundreds of million years (Teixeira et al., 2012, 2015; Ávila et al., 2014). Thus, few Archaean Lu-Hf T_{DM} ages in zircons from plutonic rocks of the Mineiro Belt are derived from cratonic areas. Indeed, Palaeoproterozoic zircon T_{DM} ages are as old as both detrital and igneous zircons from Archaean domains (Moreira et al., 2016; Martínez Dopico et al., 2017). Moreover, U-Pb and Lu-Hf analyses of detrital zircons of the syn-orogenic Sabará Group have ages between 2300 Ma and 2100 Ma and ε_{Hf}(t) from ca. +7.0 to −9.0 (Martínez Dopico et al., 2017). Therefore, the negative ε_{Hf} values are interpreted either as reworked zircon grains derived from Archaean materials or minor crustal assimilation (e.g. Woodhead et al., 2001; Nebel et al., 2011; Teixeira et al., 2015).

6.2. Metamorphic and multiple stage history of the Mineiro Belt

The magmatic-tectono-metamorphic evolution of the Mineiro Belt is poorly understood. Regional greenschist to amphibolite facies metamorphism is documented as the evidence of collision between the Palaeoproterozoic plutonic arcs and the Archaean core

of the SFC (Ávila et al., 2010, 2014; Barbosa et al., 2015). The significance of young ages in relation to older crystallised bodies is not clear, although rim ages of 2130 Ma surrounding older zircon cores (ca. 2350 Ma) has been previously reported and interpreted as metamorphic domains (Teixeira et al., 2015). Zircon is commonly the preferred mineral for U-Pb isotope studies aimed at determining the age of crystallisation of granitoid rocks, because of its resistance to thermal resetting (e.g. Schaltegger and Davies, 2017). However, zircon rims from this study (samples 16-RC1-A and 16-RC-3A) define a typical trend of variable degrees of Pb-loss, caused either by radiation damage (e.g. Cherniak et al., 1991), or by recrystallisation under metamorphic conditions (e.g. Pidgeon, 1992) and consequently an intercept age with a substandard MSWD of 82 (see Supplementary material A). Previous interpretations of metamorphic age were based on Pb loss, low Th/U and more radioactive nuclei that are significantly older (Teixeira et al., 2015). Zircon rims also have high U concentration (ca. 800 ppm on average), reflected in dark CL images, which contributed to metamictization and Pb-loss (e.g. Geisler et al., 2002). To clarify these points, titanite is an ideal geochronometer due its comparatively low closure temperature (ca. 650 °C, Pidgeon et al., 1996). This closure either indicates cooling of an igneous system or high grade metamorphic event (>650 °C) (Frost et al., 2000). Additionally, titanite analyses yielded in this study have a more reliable MSWD when compared to zircon rims (due to scattering by Pb-loss in the latter).

U-Pb analyses on titanite grains of sample 16-RC1-A yielded a concordia age of 2148 ± 6 Ma which is equal within uncertainty to the upper intercept age of zircon rims from the same sample (Fig. 4c). The question still remains whether this age represents a metamorphic overprint of rocks crystallised at 2350 Ma (core ages) or igneous crystallisation age meaning the older cores represent inherited zircons. Given the discrepancy in the Lu-Hf analyses of this work and the more evolved character of the Resende Costa Suite, the authors are inclined to the inheritance hypothesis. The Resende Costa trondhjemites zircon grains have ε_{Hf}(2350Ma) divided into two groups, consistent with juvenile (+4.2 and +1.0) and reworked zircon grains (−2.9 to −9.2), in which the second represents involvement of subducted sedimentary material (Teixeira et al., 2015). Secondly, Th/U ratios of zircon rims, albeit undeniably lower than zircon cores, are in general above 0.1 and variable (up to 0.4). Titanite grains have a relatively constant Th/U composition probably reflecting growth at chemical equilibrium with the local mineral assemblage. Additionally, abundant zircon inclusions in titanite were incorporated during crystallisation of the host, unusual in metamorphic titanites. Kohn, (2017) pointed out that metamorphic titanites grow both during prograde and retrograde metamorphism, not during peak conditions. Therefore, like zircon rims, titanites formed at lower-P during the continental arc

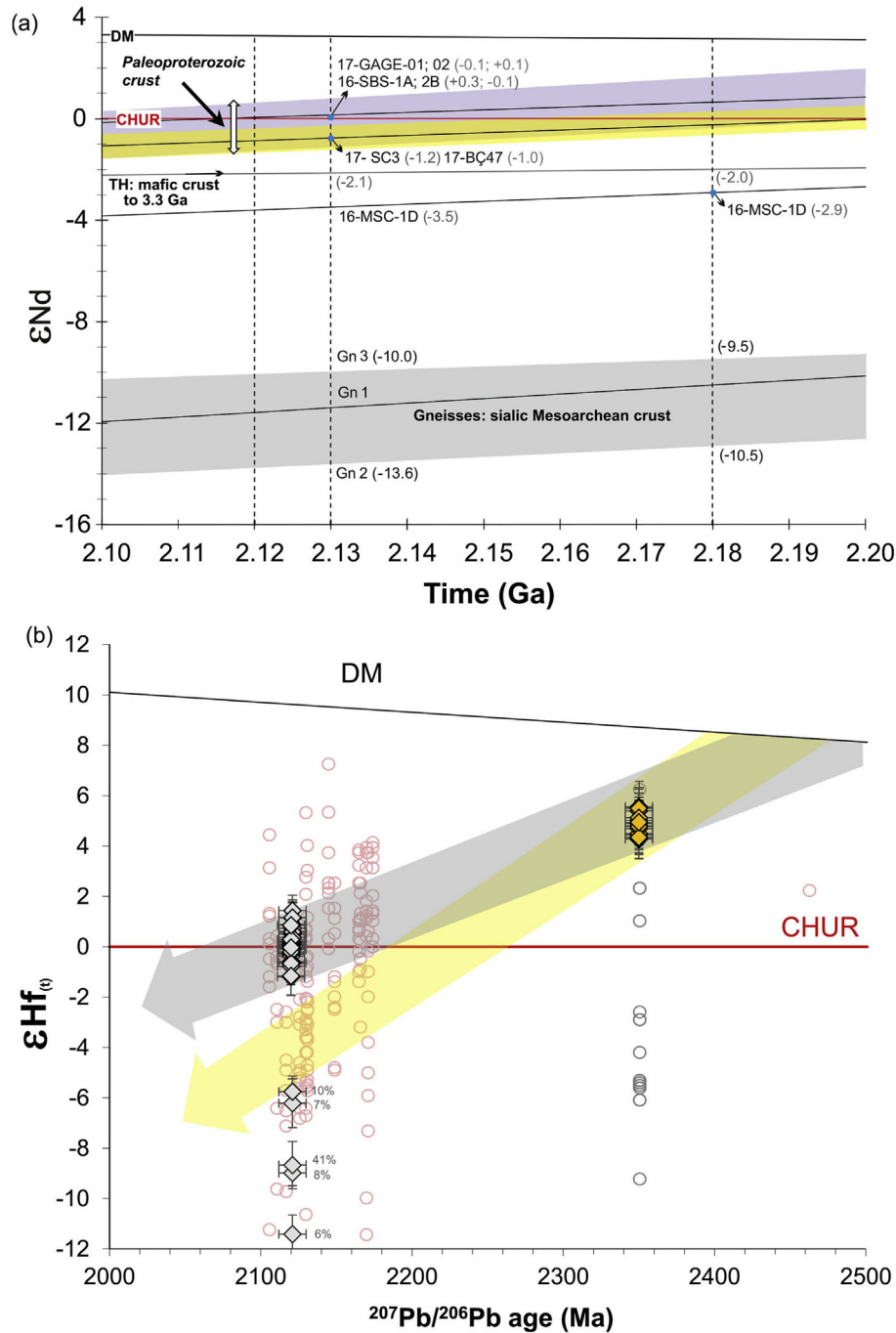


Figure 9. (a) ϵ_{Nd} versus age diagram for granitoid samples of this study. DM = depleted mantle model from DePaolo (1981). CHUR = Chondritic Uniform Reservoir. Also plotted evolutionary Nd isotope lines for Alto Maranhão (purple area) and Lagoa Dourada (yellow area) suites, representing Palaeoproterozoic juvenile crust; tholeiitic amphibolite from Ribeirão Água Limpa outcrop, representative of mafic crust; and intermediate to acid plutonic orthogneisses from eastern and northern terrane, representing Mesoproterozoic sialic crust (data from Seixas et al., 2012, 2013). Data from Table 4. (b) $\epsilon_{\text{Hf}}(t)$ against $^{207}\text{Pb}/^{206}\text{Pb}$ ages diagram. Data from samples 17-2130, 14-SCT-01 (grey diamonds) and LD5 (yellow diamonds). Pink and grey dots correspond to analyses from Barbosa et al. (2015) and Teixeira et al. (2015), respectively. Grey numbers point out the discordance percentage of U-Pb analyses justifying the few negative ϵ_{Hf} values. CHUR constants of Bouvier et al. (2008; $^{176}\text{Hf}/^{177}\text{Hf} = 0.282785$ and $^{176}\text{Lu}/^{177}\text{Hf} = 0.0336$) and T_{DM} constants of Blichert-Toft and Puchtel (2010; $^{176}\text{Hf}/^{177}\text{Hf} = 0.283294$ and $^{176}\text{Lu}/^{177}\text{Hf} = 0.03933$) were used for calculation of $\epsilon_{\text{Hf}}(t)$, CHUR and depleted mantle evolution trend (DM).

stage (Kohn et al., 2015). Thus, remelting of intermediate portions of Lagoa Dourada Suite (ca. 62 wt.% SiO_2) explains the decoupling effect witnessed in these samples and the presence of ca. 2350 Ma zircon cores. If so, the Resende Costa Suite crystallised much later, at 2148 ± 6 Ma, given the crystallisation age of the titanite grains and zircon rims (Table 2).

The youngest age defined by some zircon rims and a few titanite grains is around 2050 Ma (Table 4). This same age was reported in

monazite and titanite from a broad variety of rocks surrounding the Archaean core of the SSFC (Aguilar Gil et al., 2017); in zircon rims from the Kinawa migmatite (2034 ± 32 Ma; 2048 ± 24 Ma – Carvalho et al., 2016, 2017); and in the Itapicirica graphite schist, formed during migmatization/granulite metamorphism of carbonate sedimentary rocks at ca. 2000 Ma (Teixeira et al., 2017b). Titanite ages near 2000 Ma are related to the collapse of the Minas Orogen, which affected the Archaean and Palaeoproterozoic

domains during formation of the dome-and-keel architecture in the QF (Marshak et al., 1997; Alkmim and Marshak, 1998; Aguilar Gil et al., 2017). The data suggest that collapse affected the older Archaean basement and the orogen itself. Final evolution of the Mineiro Belt is composed of two phases: (1) collisional stage at ca. 2130 Ma to 2100 Ma (second metamorphic event of Ávila et al., 2010) and (2) collapse and slow cooling at ca. 2050 Ma to 1950 Ma, incorporating the third metamorphic event of Ávila et al. (2010), and data from Aguilar Gil et al. (2017). The short time between them is explained as rapid relaxation of the crust, not onset of a rift basin. Breakup occurred between 1800 and 1700 Ma, when the Espinhaço Supergroup and the mafic dykes of the QF first appeared (Marshak and Alkmim, 1989; Almeida et al., 2000; Cederberg et al., 2016). The two youngest sedimentary units of the QF are consistent with these observations. First, the main source of the Sabará Group (Dorr, 1969; Machado et al., 1996) comes from the Minas Orogen and reflects the change in tectonic regime as the orogen evolved and the SSFC craton acted as the foreland to flysch-type deposition (Alkmim and Martins-Neto, 2012). The maximum depositional age of the sequence is given by a zircon ID-TIMS age of 2125 ± 4 Ma (Machado et al., 1996) coeval with the main collisional stage of the belt against the Archaean portion of the craton. The second sedimentary unit, the Itacolomi Group, lies unconformably on top of the Minas Supergroup and corresponds to an intramontane molasse basin deposited during the Minas Orogen collapse (Hartmann et al., 2006; Alkmim and Martins-Neto, 2012) after 2058 ± 9 Ma (Alkmim et al., 2014). Accordingly, this age matches with the youngest zircon and titanite ages of this study. Likely, titanite first crystallised during the magma cooling and later thermal overprint due to the Mineiro Belt collapse.

6.3. Building continental crust during the magmatic lull – the geochemical evolutionary trend

The Mineiro Belt is a natural laboratory for the understanding of crustal evolution during the Palaeoproterozoic, because it contains a rare occurrence of juvenile Siderian TTGs on Earth and because of the composition of granitoids that vary through time and space. At this unique geological time, Earth was dominated by hot and shallow subduction (e.g. Dhuime et al., 2012; Hawkesworth et al., 2016), increasing oxygen levels in the atmosphere (e.g. Catling et al., 2005) and a rare set of island arcs occupied Earth's oceanic lithosphere. In this respect, the study area of this work and three other TTG island arc-like magmas were generated in the Siderian period in Brazil.

Macambira et al. (2009) reported in the Amazonian Craton 2.36 Ga juvenile intermediate rocks with $\epsilon_{\text{Nd}}(t)$ from -0.87 to $+0.78$ and some other granitoids with similar signatures. Dos Santos et al. (2009) described analogous occurrences in the western portion of the Borborema Province where ca. 2.35 Ga granodioritic gneisses have positive $\epsilon_{\text{Nd}}(t)$ and an island arc seems the most likely tectonic setting. Also, Girelli et al. (2016) reported juvenile granodiorites of the Santa Maria Chico Granulitic Complex, in the Rio de La Plata Craton, southern Brazil, for which zircon ages range from 2.38 Ga to 2.28 Ga with positive $\epsilon_{\text{Hf}}(t)$ between $+0.29$ and $+9.64$. These island arcs, similar to the tectonic evolution of the Mineiro Belt, collided against Archaean cratonic areas at ca. 2.1 Ga (Vasquez et al., 2008; Dos Santos et al., 2009; Santos et al., 2003). In Brazil, the collage of Archaean and accreted Palaeoproterozoic terranes at this time is defined as the Transamazonian Orogeny (for the Amazonian Craton) or Minas accretionary orogeny (for the SFC) (Alkmim and Marshak, 1998; Teixeira et al., 2015, 2017a). Globally, other occurrences of juvenile TTG suites have been reported in Canada, China, Australia and West Africa (for details see compilation of Partin et al., 2014 and references therein).

Chronologically, older granitoids in the Mineiro Belt are less enriched in Ba and Sr than the younger rocks. For example, the Lagoa Dourada Suite (ca. 2350 Ma) is depleted in Ba + Sr, rarely possessing more than 700 ppm and characterised by $\text{Sr/Ba} > 1.5$. Similarly, sample 16-MS-C-1D is dated at 2180 Ma and is 40%–50% less enriched in Ba + Sr than the ca. 2130 Ma granitoids, which have significantly more enriched concentrations (Fig. 5a–c). Nevertheless, the ca. 2130 Ma granitoids are not sanukitoids/adakites as the Alto Maranhão Suite is. However, geochemically they all sit between sanukitoid and hybrid granites *sensu* Laurent et al. (2014) (Fig. 8). These Palaeoproterozoic 'hybrid' magmas were initially described as miscellaneous by Seixas et al. (2012, 2013) or broadly incorporated as the Alto Maranhão Suite, Ritópolis batholith and coeval rocks (Barbosa et al., 2015; Teixeira et al., 2015; Alkmim and Teixeira, 2017). In this study, they are interpreted as a ca. 2130 Ma juvenile high Ba–Sr suite. This group is distinguished from the Alto Maranhão Suite (after the definition of Seixas et al., 2013) by low concentrations of compatible elements (i.e. Cr, Ni and Mg#) (Figs. 5d and 7d). Even so, the absence of crustal reworking in the genesis of the juvenile Ba–Sr suite causes the resemblance with the sanukitoids, rather than being similar to the hybrid granitoids *sensu stricto* of Laurent et al. (2014). The coeval age of the plutons, the similar geochemistry (but with relative depletion in Mg#, Cr and Ni) and the Sm–Nd isotopic signature can be used to incorporate these occurrences into the Alto Maranhão Suite. If so, the area of exposed juvenile high Ba–Sr magmatism is up to 500 km², with 300 km² defined as the sanukitoid suite (i.e. Alto Maranhão Suite). Comparable with the Alto Maranhão Suite, these coeval plutons were derived from a similar juvenile source with a slightly higher degree of fractional crystallisation and little assimilation of older crustal rocks. Alternatively, they could have been derived from a different source, whereby the miscellaneous tonalites were not sourced from the metasomatised mantle, but from a lower portion of the crust above the mantle wedge.

Therefore, Siderian–Rhyacian evolution stage of the Mineiro Belt was akin to high Ba–Sr magmas (e.g. Tarney and Jones, 1994; Fowler and Rollinson, 2012; Laurent et al., 2014) and resembles the Archaean–Palaeoproterozoic transition from TTG to sanukitoid magmas (e.g. Martin and Moyen, 2002; Halla et al., 2017). Thus, delayed geochemical transition occurred compared to other cratonic areas in the continents (Laurent et al., 2014; Halla et al., 2017), also supported by a lack of this secular geochemical transformation in the Archaean nucleus of the SFC (Figs. 2 and 8).

6.4. Implications and future evaluation of the magmatic lull

Depleted mantle model ages are debated as to whether they represent real ages and direct measure of the timing of juvenile crust addition to the continents (e.g. Payne et al., 2016). However, uncertainties related to model ages do not disrupt the overall shape and meaning of the calculated crustal growth curve based on large datasets (Dhuime et al., 2017). In the following, we present a compilation of 2067 Lu–Hf analyses published so far both in igneous and detrital zircons of the QF and Mineiro Belt, plotted as crustal residence time versus age (Fig. 10). Model ages are used in calculations simply by subtracting their values from crystallisation ages and the results represent a rough estimation of crustal residence time (e.g. Griffin et al., 2006). Thus, the presented diagram is considered in its qualitative meaning and general sense (Vervoort and Kemp, 2016). Blue and grey dots display negative $\epsilon_{\text{Hf}}(t)$, while red dots are positive. Respectively, red and grey linear functions are composed of positive and negative $\epsilon_{\text{Hf}}(t)$ and depict different gradients. Red dots appear to oscillate regularly through time, although defining a shallow slope towards younger ages. In fact, juvenile compositions result in restricted residence times and a low slope (0.0982 ± 0.002),

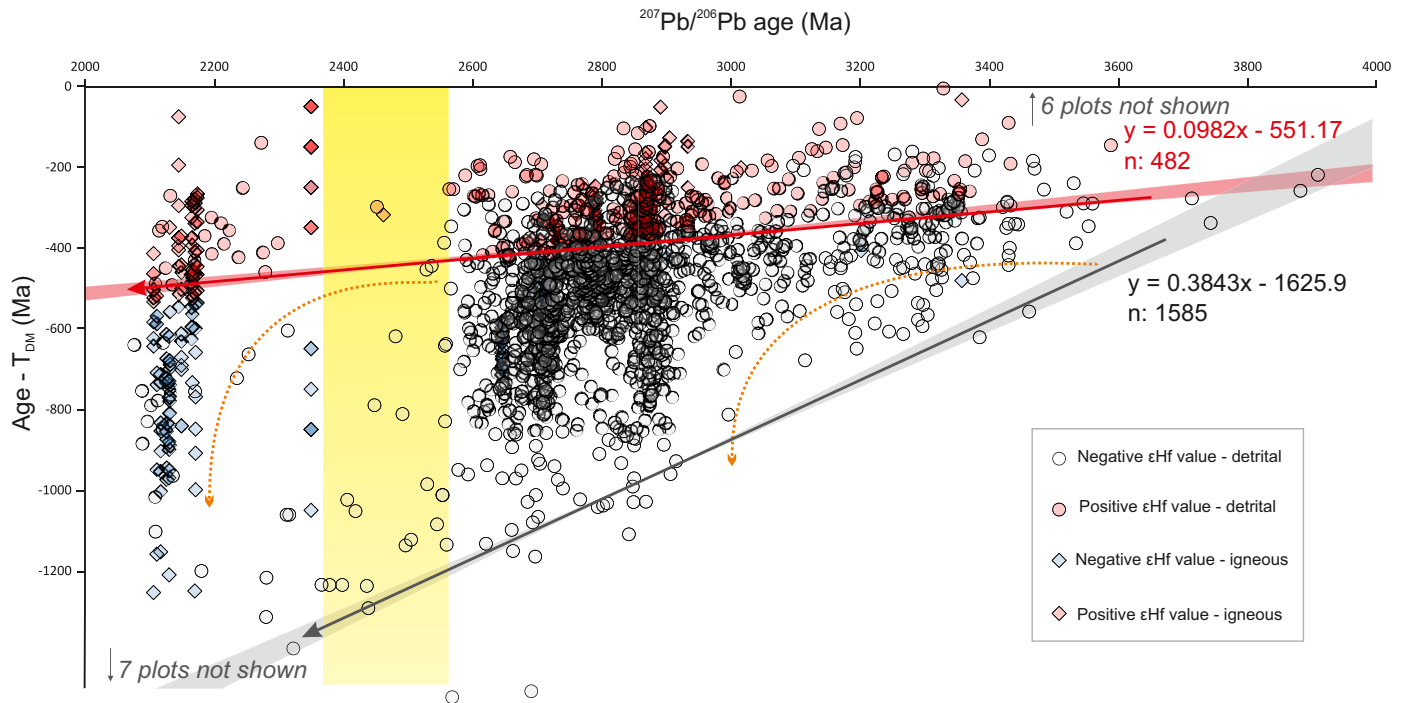


Figure 10. Compilation of 2067 U–Pb–Hf analyses of detrital and igneous zircons from the QF and Mineiro Belt (Barbosa et al., 2015; Teixeira et al., 2015; Albert et al., 2016; Moreira et al., 2016; Martínez Dopico et al., 2017; this study). Crystallisation age - T_{DM} (Ma) vs. $^{207}\text{Pb}/^{206}\text{Pb}$ age (Ma) diagram shows positive $\epsilon_{\text{Hf}}(t)$ values result in restricted residence time as they represent juvenile compositions of the source magma. Grey linear function depicts greater angular coefficient than red analogue, which suggest increase of recycling process through time and relative steady juvenile addition to the crust. Two orange dashed curves suggest increase periods of crustal recycling. Ten analyses were not used for linear trends calculation because they present unrealistic crustal residence time (i.e. Crystallisation age - $T_{DM} > 0$).

whereas reworked material has a broader residence time and a steeper slope (0.3843 ± 0.008). The yellow interval in the diagram shows a pause of ca. 200 Ma followed by addition of juvenile magmas into the crust (Fig. 10). A repetition of TTG magma production occurred in the region at this stage as shown previously in Fig. 2. Similarly, the two periods were followed by an increase in crustal recycling, highlighted by the orange lines, with an inflexion shortly after juvenile magma additions. Increase of recycling seen in the Archaean was associated with the collisional system and continent amalgamation (e.g. Moreira et al., 2016; Martínez Dopico et al., 2017), while in the Palaeoproterozoic it was associated with the Mineiro Belt collision against the cratonic margins at ca. 2100 Ma. Indeed, ϵ_{Hf} values in zircon become increasingly enriched (lower ϵ_{Hf}) towards collisional/compressional phases in peripheral orogenic settings (e.g. Roberts and Spencer, 2015).

A diminishing number of ages between 2.6 Ga and 2.4 Ga is apparent. The lack of data during this interval of almost 200 Ma is mainly due to a decrease in magmatism. Characterization of ca. 2650 Ma A-type magmatism in the western region of the QF (Moreno et al., 2017) corresponds to breakup after lithospheric stabilization (Condie et al., 2015). Supercontinent fragmentation, together with the emergence of Wilson cycle-type sedimentation, preceded the tectonic evolution of SSFC as controlled by successive accretion of magmatic arcs, stabilization and rifting (e.g. Alkmim and Marshak, 1998; Alkmim and Teixeira, 2017; Martínez Dopico et al., 2017).

An increasing number of magmatic occurrences in the last few years are within the magmatic lull. Kenorland supercontinent assembly is the best option to explain the dearth of magmatism in this period (Lubnina and Slabunov, 2011; Pehrsson et al., 2014). Indeed, this hypothesis explains important points regarding Earth's tectono-thermal conditions and convincingly suggests that plate tectonics did not stop. However, it does not explain the particular geochemistry and isotopic signature of the magmas generated within the interval, nor

why the same magma-type is not recurrent as a consequence of other continental amalgamations during different periods (e.g. Condie, 2016; Lawley, 2016). Recent Palaeoproterozoic geodynamic reconstruction of the SFC-Congo Craton has been proposed based on magmatic and metamorphic comparisons with the North China blocks (Cederberg et al., 2016; Teixeira et al., 2017b). Additional isotopic information is required to formulate a global tectonic model during the Siderian–Rhyacian interval. For example, a thorough investigation of variations in high Ba–Sr magmas coupled with a broader dataset of oxygen isotope and trace element analyses in mineral accessory phases could better characterize mantle derived contributions and constrain the evolution of the subcontinental lithosphere and continental crust growth rates (e.g. Hawkesworth and Kemp, 2006; Dhuime et al., 2012; Heilimo et al., 2013).

7. Conclusions

The Mineiro Belt is composed of a set of arcs. The older arcs (>2.3 Ga) have plutonic rocks with more characteristic juvenile Hf–Nd signatures and depletion of Ba–Sr when compared to younger occurrences in the Mineiro Belt (ca. 2.2–2.1 Ga). Geochemical data suggest an igneous differentiation mechanism for the plutons. The lack of significant Eu anomalies in the REE patterns argues for a genetic link of the granitoids with the mafic magmas of the Mineiro Belt. The high Ba and Sr of most ca. 2.13 Ga samples is consistent with a subduction stage as a factor controlling the sanukitoid geochemical signature of the 2.13 Ga Alto Maranhão Suite. Magmas coevally emplaced in the Alto Maranhão Suite are envisaged as formed by underplating melt, above the mantle wedge (e.g. Petford and Atherton, 1996). Alternatively, they were derived from a subsequent melt of the Alto Maranhão Suite source and therefore have lower concentrations of compatible elements. The interval between T_{DM} and crystallisation ages and a small input of inherited older

zircons, associated with Pb anomalies, suggests minor crustal involvement during the genesis of the Mineiro Belt. Coeval crustal-like magmas were potentially formed during collisional stages in active continental margin settings (Barbosa et al., 2015). The overall evolution of the Mineiro Belt seems akin to the secular evolution of granitoids at the Archaean–Palaeoproterozoic boundary. Such correlation implies a late transition from TTG to sanukitoid magmatism starting within the magmatic lull in this region. The hybrid granitoids presented in this study are different, however, to the Archaean hybrid granites defined by Laurent et al. (2014). This is because the rocks of the Mineiro Belt have a smaller amount of older crust involved in their genesis as demonstrated by the Hf–Nd analyses, particularly for the 2.35 Ga Lagoa Dourada Suite. We suggest the presence of an extended passive margin, with dispersed island arcs that eventually collided against the Archaean craton, ultimately leading to the amalgamation of the São Francisco palaeocontinent. The results of the present study shed new light on the global distribution of TTG magmas during a distinct tectonic scenario of Earth's crustal evolution.

Acknowledgements

H. Moreira thanks CNPq (National Counsel of Technological and Scientific Development, Brazil) grant (234610/2014-0); R. Parrish for enlightening discussions about U–Pb titanite data; and G. Gonçalves for collaboration at the beginning of this project. L. Seixas thanks CAPES (Brasília, Brazil), FAPEMIG (Belo Horizonte, Brazil), UFOP (Ouro Preto, Brazil), UPS/Laboratoire de Volcanologie–Pétrographie (Orsay, France) and UQAM/GEOTOP (Montreal, Canada) for support during the early stages of this research. C. Lana acknowledges APQ-3793-16 project funding. W. Teixeira, L. Hartmann and an anonymous reviewer are acknowledged for constructive comments which greatly improved this manuscript. Authors thank C. Spencer and R. Palin for the invitation to contribute to this special issue.

Appendix A. Supplementary data

Supplementary data related to this article can be found at <https://doi.org/10.1016/j.gsf.2018.01.009>.

References

- Aguilar Gil, C., Alkmim, F.F., Lana, C., Farina, F., 2017. Paleoproterozoic assembly of the São Francisco craton, SE Brazil: new insights from U–Pb titanite and monazite dating. *Precambrian Research* 289, 95–115.
- Albert, C., Farina, F., Lana, C., Stevens, G., Storey, C., Gerdes, A., Martínez Dopico, C., 2016. Archaean crustal evolution in the southern São Francisco Craton, Brazil: constraints from U–Pb, Lu–Hf and O isotope analyses. *Lithos*. <https://doi.org/10.1016/j.lithos.2016.09.029>.
- Alkmim, F.F., Lana, C., Duque, T.R.F., 2014. Zircões detríticos do Grupo Itacolomi e o registro do soerguimento do cinturão Mineiro. 47° Congresso Brasileiro de Geologia. Salvador, Brasil. Anais CD-ROM, p. 1802.
- Alkmim, F.F., Noce, C.M., 2006. Outline of the geology of Quadrilátero Ferrífero. In: Alkmim, F.F., Noce, C.M. (Eds.), *The Paleoproterozoic Record of São Francisco Craton*. IGCP 509 Field Workshop, pp. 37–73. Bahia and Minas Gerais (Field Guide and Abstracts).
- Alkmim, F.F., Teixeira, W., 2017. The paleoproterozoic Mineiro belt and the Quadrilátero Ferrífero. In: Heilbron, M., Alkmim, F., Cordani, U.G. (Eds.), *The São Francisco Craton and its Margins, Eastern Brazil*, *Geology Review Series*. Springer-Verlag, pp. 71–94. https://doi.org/10.1007/978-3-319-01715-0_5 chapter 5.
- Alkmim, F.F., Marshak, S., 1998. The transamazonian orogeny in the quadrilátero-ferrífero, Minas gerais, Brazil: paleoproterozoic collision and collapse in the southern São Francisco craton region. *Precambrian Research* 90, 29–58.
- Alkmim, F.F., Martins-Neto, M.A., 2012. Proterozoic first-order sedimentary sequences of the São Francisco Craton, eastern Brazil. *Marine and Petroleum Geology* 33, 127–139.
- Almeida, F.F.M., Brito Neves, B.B., Carneiro, C.D.R., 2000. The origin and evolution of the south American Platform. *Earth Science Reviews* 50, 77–111.
- Arndt, N., Davaille, A., 2013. Episodic earth evolution. *Tectonophysics* 609, 661–674. <https://doi.org/10.1016/j.tecto.2013.07.002>.
- Ávila, C.A., Teixeira, W., Cordani, U.G., Moura, C.A.V., Pereira, R.M., 2010. Rhyacian (2.23–2.20 Ga) juvenile accretion in the southern São Francisco craton, Brazil: geochemical and isotopic evidence from the Serrinha magmatic suite, Mineiro belt. *Journal of South American Earth Sciences* 29, 464–482.
- Ávila, C.A., Teixeira, W., Bongioiolo, E.M., Dussin, I.A., 2014. The Tiradentes suite and its role in the Rhyacian evolution of the Mineiro belt–São Francisco Craton: geochemical and U–Pb geochronological evidences. *Precambrian Research* 243, 221–251.
- Baltazar, O.F., Zucchetti, M., 2007. Lithofacies associations and structural evolution of the Archaean Rio das Velhas greenstone belt, Quadrilátero Ferrífero Brazil: a review of the setting of gold deposits. *Ore Geology Reviews* 32, 1–2.
- Barbosa, J.S.F., Sabatê, P., 2004. Archaean and paleoproterozoic crust of the São Francisco craton, Bahia, Brazil: geodynamic features. *Precambrian Research* 133, 1–27.
- Barbosa, N.S., 2015. Evolução Paleoproterozoica do Cinturão Mineiro: Geocronologia U–Pb, isótopos de Nd–Hf–Sr e geoquímica de rochas plutônicas. PhD Thesis. Universidade de São Paulo, p. 229.
- Barbosa, N., Teixeira, W., Ávila, C.A., Montecinos, P.M., Bongioiolo, E.M., Vasconcelos, F.F., 2018. U–Pb geochronology and coupled Hf–Nd–Sr isotopic-chemical constraints of the Cassiterita Orthogneiss (2.47–2.41 Ga) in the Mineiro belt, São Francisco craton: Geodynamic fingerprints beyond the Archaean–Paleoproterozoic Transition. *Precambrian Res.* <https://doi.org/10.1016/j.precamres.2018.01.017>.
- Barbosa, N.S., Teixeira, W., Ávilac, C.A., Montecinos, P.M., Bongioiolo, E.M., 2015. 2.17–2.10 Ga plutonic episodes in the Mineiro belt, São Francisco Craton, Brazil: U–Pb ages, geochemical constraints and tectonics. *Precambrian Research* 270, 204–225.
- Barker, F., 1979. Trondhjemite: definition, environment and hypotheses of origin. In: Barker, F. (Ed.), *Trondhjemites, Dacites and Related Rocks*. Elsevier, New York, pp. 1–12.
- Boynton, W.V., 1984. Cosmochemistry of the rare earth elements: meteorite studies. In: Henderson, P. (Ed.), *Rare Earth Element Geochemistry (Developments in Geochemistry 2)*. Elsevier, Amsterdam, pp. 63–114.
- Carneiro, M.A., 1992. O Complexo Metamórfico Bonfim Setentrional (Quadrilátero Ferrífero, Minas Gerais): Litoestratigrafia e evolução geológica de um segmento de crosta continental do Arqueano (Unpublished PhD Thesis). University of São Paulo, Brazil, p. 233.
- Carvalho, B.B., Sawyer, E.W., Janasi, V.A., 2016. Crustal reworking in a shear zone: transformation of metagranite to migmatite. *Journal of Metamorphic Geology* 34, 237–264.
- Carvalho, B.B., Janasi, V.A., Sawyer, E.W., 2017. Evidence for Paleoproterozoic anatexis and crustal reworking of Archaean crust in the São Francisco Craton, Brazil: a dating and isotopic study of the Kinawa migmatite. *Precambrian Research* 291, 98–118. <https://doi.org/10.1016/j.precamres.2017.01.019>.
- Catling, D.C., Glein, C.R., Zahnle, K.J., McKay, C.P., 2005. Why O₂ is required by complex life on habitable planets and the concept of planetary “oxygenation time”. *Astrobiology* 5 (3), 415–438.
- Cawood, P.A., Alfred Kröner, Collins, William J., Kusky, Timothy M., Mooney, Walter D., Windley, Brain F., 2009. Accretionary orogens through Earth's history. Geological Society, London, Special Publications 318 (1), 1–36. <https://doi.org/10.1144/SP318.1>.
- Cawood, P.A., Hawkesworth, C.J., Dhuime, B., 2013. The continental record and the generation of continental crust. *Geological Society of America Bulletin* 125 (1–2), 14–32. <https://doi.org/10.1130/B30722.1>.
- Cederberg, J., Söderlund, U., Oliveira, E.P., Ernst, R.E., Pisarevsky, S.A., 2016. U–Pb baddeleyite dating of the Proterozoic Pará de Minas dyke swarm in the São Francisco Craton (Brazil) - implications for tectonic correlation with the Siberian, Congo and North China cratons. *GFF* 138, 219–240.
- Cherniak, D.J., Lanford, W.A., Ryerson, F.J., 1991. Lead diffusion in apatite and zircon using ion implantation and Rutherford backscattering techniques. *Geochimica et Cosmochimica Acta* 55, 1663–1673.
- Condie, K.C., 2005. TTGs and adakites: are they both slab melts? *Lithos* 80, 33–44.
- Condie, K.C., Pease, V. (Eds.), 2008. When did plate tectonics start on Planet Earth?. *Geological Society of America Special Paper*, 440, pp. 1–29.
- Condie, K.C., O'Neill, C., Aster, R.C., 2009. Evidence and implications for a widespread magmatic shutdown for 250 My on Earth. *Earth and Planetary Science Letters* 282, 294–298.
- Condie, K.C., Davaille, A., Aster, R.C., Arndt, N., 2015. Upstairs-downstairs: supercontinents and large igneous provinces, are they related? *International Geology Review* 57 (11e12), 1341–1348.
- Condie, K.C., 2016. A planet in transition: the onset of plate tectonics on Earth between 3 and 2 Ga?. *Geoscience Frontiers* 9 (1), 51–60. <https://doi.org/10.1016/j.gsf.2016.09.001>.
- Cox, K.G., Bell, J.D., Pankhurst, R.J., 1979. The interpretation of igneous rocks. *Allen and Unwin*, London, 450 p.
- DePaolo, D.J., 1981. Neodymium isotopes in the Colorado Front Range and crust–mantle evolution in the Proterozoic. *Nature* 291, 193–196.
- Dhuime, B., Wuestefeld, A., Hawkesworth, C.J., 2015. Emergence of modern continental crust about 3 billion years ago. *Nature Geosciences* 8, 552–555.
- Dhuime, B., Hawkesworth, C.J., Cawood, P.A., Storey, C.D., 2012. A change in the geodynamics of continental growth 3 billion years ago. *Science* 335, 1334–1336. <https://doi.org/10.1126/science.1216066>.
- Dhuime, B., Hawkesworth, C.J., Delavault, H., Cawood, P.A., 2017. Continental growth seen through the sedimentary record. *Sediment. Geol.* 357, 16–32. <https://doi.org/10.1016/j.sedgeo.2017.06.001>.

- Dorr II, J.V.N., 1969. Physiographic, Stratigraphic and Structural Development Of the Quadrilátero Ferrífero, Minas Gerais, Brazil. USGS/DNPM, Washington Professional Paper 641-A, p. 110.
- Dos Santos, T.J., Fetter, A.H., Van Schmus, W.R., Hackspacher, P.C., 2009. Evidence for 2.35 to 2.30 Ga juvenile crustal growth in the northwest Borborema Province, NE Brazil. *Geological Society, London, Special Publications* 323, 271–281.
- Drummond, M.S., Defant, M.J., 1990. A model for trondhjemite–tonalite–dacite gen-esis and crustal growth via slab melting: Archean to modern comparisons. *Journal of Geophysical Research* 95, 21503–21521.
- Ernst, W.G., 2017. Kimberlites and the start of plate tectonics – Comment. *Geology* 45, e405. <https://doi.org/10.1130/G38681C.1>.
- Farina, F., Albert, C., Lana, C., 2015. The Neoproterozoic transition between medium and high-K granitoids: clues from the Southern São Francisco Craton (Brazil). *Precambrian Research* 266, 375–394.
- Farina, F., Albert, C., Martínez Dopico, C., Aguiar Gil, C., Moreira, H., Hippertt, J.P., Cutts, K., Alkmim, F.F., Lana, C., 2016. The Archean–Paleoproterozoic evolution of the Quadrilátero Ferrífero (Brasil): current models and open questions. *Journal of South American Earth Sciences* 68, 4–21.
- Flament, N., Coltice, N., Rey, P.F., 2008. A case for late-Archaean continental emergence from thermal evolution models and hypsometry. *Earth and Planet Science Letters* 275, 326–336.
- Fowler, M.B., Rollinson, H., 2012. Phanerozoic sanukitoids from caledonian scotland: implications for archaean subduction. *Geology* 40 (12), 1079–1082.
- Frost, B.R., Chamberlain, K.R., Schumacher, J.C., 2000. Sphene (titanite): phase relations and role as a geochronometer. *Chemical Geology* 172, 131–145.
- Geisler, T., Pidgeon, R., van Bronswijk, W., Kurtz, R., 2002. Transport of uranium, thorium, and lead in metamict zircon under low-temperature hydrothermal conditions. *Chemical Geology* 191, 41–154.
- Gerya, T.V., Stern, R.J., Baes, M., Sobolev, S.V., Whattam, S.A., 2015. Plate tectonics on the earth triggered by plume-induced subduction initiation. *Nature* 527, 221–225.
- Girelli, T.J., Chemale Jr., F., Lavina, E.L.C., Laux, J.H., Bongiolo, E., Lana, C., 2016. Proterozoic Evolution of Santa Maria Chico Granulitic Complex and Adjacent Areas. 8^o Congresso Uruguayo de Geologia, Montevideu.
- Griffin, W.L., Belousova, E.A., Walters, S.G., O'Reilly, S.Y., 2006. Archean and Proterozoic crustal evolution in the Eastern Succession of the Mt Isa district, Australia: U–Pb and Hf-isotope studies of detrital zircons. *Australian Journal of Earth Science* 53, 125–149.
- Halla, J., Whitehouse, M.J., Ahmad, T., Bagai, Z., 2017. Archaean granitoids: an overview and significance from a tectonic perspective. *Geological Society, London, Special Publications* 449, 1–18.
- Halla, J., van Hunen, J., Heilimo, E., Hölttä, P., 2009. Geochemical and numerical constraints on Neoproterozoic plate tectonics. *Precambrian Research* 174, 155–162.
- Hartmann, L.A., Endo, I., Suita, M.T.F., Santos, J.O.S., Frantz, J.C., Carneiro, M.A., Naughton, N.J., Barley, M.E., 2006. Provenance and age delimitation of Quadrilátero Ferrífero sandstones based on zircon U–Pb isotopes. *Journal of South American Earth Sciences* 20, 273–285.
- Hawkesworth, C., Cawood, P., Dhuime, B., 2016. Tectonics and crustal evolution. *GSA Today* 26, 4–11. <https://doi.org/10.1130/GSATG272A.1>.
- Hawkesworth, C.J., Kemp, A.I.S., 2006. Using hafnium and oxygen isotopes in zircons to unravel the record of crustal evolution. *Chemical Geology* 226, 144–162. <https://doi.org/10.1016/j.chemgeo.2005.09.018>.
- Heilbron, M., Duarte, B.P., Valeriano, C.M., Simonetti, A., Machado, N., Nogueira, J.R., 2010. Evolution of reworked Paleoproterozoic basement rocks within the Ribeira belt (Neoproterozoic), SE-Brazil, based on U–Pb geochronology: Implications for paleogeographic reconstructions of the São Francisco-Congo paleocontinent. *Precambrian Res.* 178, 136–148.
- Heilimo, E., Halla, J., Andersen, T., Huhma, H., 2013. Neoproterozoic crustal recycling and mantle metasomatism: Hf–Nd–Pb–O isotope evidence from sanukitoids of the Fennoscandian shield. *Precambrian Research* 228, 250–266.
- Horstwood, M.S.A., Köslér, J., Gehrels, G., Jackson, S.E., McLean, N.M., Paton, C., Pearson, N.J., Sircombe, K., Sylvester, P., Vermeesch, P., Bowring, J.F., Condon, D.J., Schoene, B., 2016. Community-derived standards for LA-ICP-MS U–Th–Pb geochronology – uncertainty propagation, age interpretation and data reporting. *Geostandards and Geoanalytical Research* 40, 311–332.
- Kohn, M.J., 2017. Titanite petrochronology. *Reviews in Mineralogy and Geochemistry* 83 (1), 419–441.
- Kohn, M.J., Corrie, S.L., Markley, C., 2015. The fall and rise of metamorphic zircon. *American Mineralogist* 100, 897–908.
- Korenaga, J., 2013. Initiation and evolution of plate tectonics on earth: theories and observations. *Annual Reviews of Earth and Planetary Sciences* 41, 117–151.
- Lana, C., Alkmim, F.F., Armonstrong, R., Scholz, R., Romano, R., Nalini Jr., H.R., 2013. The ancestry and magmatic evolution of Archaean TTG rocks of the Quadrilátero Ferrífero province, Southeast Brazil. *Precambrian Research* 231, 157–173.
- Laurent, O., Martin, H., Moyen, J.-F., Doucelance, R., 2014. The diversity and evolution of late-Archaean granites: evidence for the onset of a “modern-style” plate tectonics between 3.0 and 2.5 Ga. *Lithos* 205, 208–235.
- Lobato, L.M., Santos, J.O.S., McNaughton, N.J., Fletcher, I.R., Noce, C.M., 2007. U–Pb SHRIMP monazite ages of the giant Morro Velho and Cuiabá gold deposits, Rio das Velhas greenstone belt, Quadrilátero Ferrífero, Minas Gerais, Brazil. *Ore Geology Reviews* 32 (3–4), 674–680.
- Lubnina, N.V., Slabunov, A.I., 2011. Reconstruction of the Kenorland supercontinent in the Neoproterozoic based on paleomagnetic and geological data. *Moscow University Geology Bulletin* 66 (4), 242–249.
- Lawley, C.J.M., 2016. Compositional symmetry between Earth's crustal building blocks. *Geochemical Perspectives Letters* 2, 117–126.
- Macambira, M.J.B., Vasquez, M.L., da Silva, D.C.C., Galarza, M.A., Barros, C.E.deM., Camelo, J.deF., 2009. Crustal growth of the central-eastern Paleoproterozoic Bacajá domain, SE Amazonian craton: Juvenile accretion vs. reworking. *Journal of South American Earth Sciences* 27, 235–246.
- Machado, N., Schrank, A., Noce, C.M., Gauthier, G., 1996. Ages of detrital zircon from Archean–Paleoproterozoic sequences: implications for Greenstone Belt setting and evolution of a Transamazonian foreland basin in Quadrilátero Ferrífero, southeast Brazil. *Earth Planet. Sci. Lett.* 141, 259–276. [https://doi.org/10.1016/0012-821X\(96\)00054-4](https://doi.org/10.1016/0012-821X(96)00054-4).
- Marshak, S., Alkmim, F.F., 1989. Proterozoic contraction/extension tectonics of the southern São Francisco region, Minas Gerais, Brazil. *Tectonics* 8, 555–571.
- Marshak, S., Tinkham, D., Alkmim, F.F., Brueckner, H.K., Bornhorst, T., 1997. Dome and-keel provinces formed during Paleoproterozoic orogenic collapse-Diapir clusters or core complexes? Examples from the Quadrilátero Ferrífero (Brazil) and the Penokean Orogen (USA). *Geology* 25, 415–418.
- Martin, H., 1986. Effect of steeper Archean geothermal gradient on geochemistry of subduction-zone magma. *Geology* 14, 753–756.
- Martin, H., Moyen, J.F., 2002. Secular changes in TTG composition as markers of the progressive cooling of the Earth. *Geology* 30 (4), 319–322.
- Martin, H., Moyen, J.F., Rapp, R., 2010. The sanukitoid series: magmatism at the Archaean–Proterozoic transition. *Royal Society of Edinburgh Transactions* 100, 15–33. <https://doi.org/10.1017/S1755691009016120>.
- Martinez Dopico, C.L., Lana, C., Moreira, H.S., Cassino, L.F., Alkmim, F.F., 2017. U–Pb ages and Hf-isotope data of detrital zircons from the late neoproterozoic-paleoproterozoic Minas basin, SE Brazil. *Precambrian Research* 291, 143–161.
- McDonough, W.F., Sun, S.-S., 1995. The composition of the Earth. *Chemical Geology* 120, 223–253.
- Moore, W.B., Webb, A.A.G., 2013. Heat pipe earth. *Nature* 500, 501–505.
- Moreira, H., Lana, C., Nalini, H.A., 2016. The detrital zircon record of an Archaean convergent basin in the Southern São Francisco Craton, Brazil. *Precambrian Res.* 275, 84–99. <https://doi.org/10.1016/j.precambres.2015.12.015>.
- Moreno, J.A., Baldim, M.R., Semprich, J., Oliveira, E.P., Verma, S.K., Teixeira, W., 2017. Geochronological and geochemical evidences for extension-related Neoproterozoic granitoids in the southern São Francisco Craton, Brazil. *Precambrian Research* 294, 322–343.
- Moyen, J.F., Martin, H., 2012. Forty years of TTG research. *Lithos* 148, 312–336.
- Moyen, J.F., Stevens, G., Kisters, A.F.M., 2006. Record of mid-Archaean subduction from metamorphism in the Barberton terrane, South Africa. *Nature* 442, 559–562.
- Nebel, O., Vroon, P.Z., van Westrenen, W., Iizuka, T., Davies, G.R., 2011. The effect of sediment recycling in subduction zones on the Hf isotope character of new arc crust, Banda arc, Indonesia. *Earth and Planetary Science Letters* 303, 240–250.
- Noce, C.M., Teixeira, W., Queméneur, J.J.G., Martins, V.T.S., Bolzaquini, E., 2000. Isotopic signatures of Paleoproterozoic granitoids from the southern São Francisco Craton and implications for the evolution of the Transamazonian Orogeny. *Journal of South American Earth Sciences* 13, 225–239.
- Noce, C.M., Zuccheti, M., Baltazar, O.F., Armstrong, R., Dantas, E., Renger, F.E., Lobato, L.M., 2005. Age of felsic volcanism and the role of ancient continental crust in the evolution of the Neoproterozoic Rio das Velhas greenstone belt (Quadrilátero Ferrífero, Brazil): U–Pb zircon dating of volcanoclastic graywackes. *Precambrian Research* 141, 67–82.
- Noce, C.M., Pedrosa-Soares, A.C., Silva, L.C., Armstrong, R., Piuzana, D., 2007. Evolution of polycyclic basement in the Araçuaí Orogen based on U–Pb SHRIMP data: implications for the Brazil–Africa links in the Paleoproterozoic time. *Precambrian Research* 159, 60–78.
- O'Connor, J.T., 1965. A classification for quartz-rich igneous rocks based on feldspar ratios. *US Geological Survey Professional Paper* B 525, 79–84.
- O'Neill, C., Lenardic, A., Moresi, L., Torsvik, T.H., Lee, C.T.A., 2007. Episodic pre-cambrian subduction. *Earth and Planetary Science Letters* 262, 552–562.
- Payne, J.L., McInerney, D.J., Barovich, K.M., Kirkland, C.L., Pearson, N.J., Hand, M., 2016. Strengths and limitations of zircon Lu–Hf and O isotopes in modelling crustal growth. *Lithos* 248–251, 175–192.
- Partin, C.A., Bekker, A., Sylvester, P.J., Wodicka, N., Stern, R.A., Chacko, T., Heaman, L.M., 2014. Filling in the juvenile magmatic gap: evidence for uninterrupted Paleoproterozoic plate tectonics. *Earth and Planetary Science Letters* 388, 123–133.
- Pehrsson, S.J., Buchan, K.L., Eglinton, B.M., Berman, R.M., Rainbird, R.H., 2014. Did plate tectonics shutdown in the Paleoproterozoic? A view from the Siderian geochronological record. *Gondwana Research* 26 (3), 803–815.
- Peucat, J.J., Barbosa, J.S.F., Paquette, J.L., Martin, H., Fanning, C.M., Leal, A.B.M., 2011. Geochronology of granulites from the south Itabuna-Salvador-Curaçá Block, São Francisco Craton (Brazil): Nd isotopes and U–Pb zircon ages. *Journal of South American Earth Sciences* 31, 397–413.
- Petford, N., Atherton, M., 1996. Na-rich partial melts from newly underplated basaltic crust: the Cordillera Blanca Batholith, Peru. *Journal of Petrology* 37, 1491–1521.
- Pidgeon, R.T., 1992. Recrystallisation of oscillatory zoned zircon: some geochronological and petrological implications. *Contrib. Mineral. Petrol.* 110, 463–472.
- Pidgeon, R.T., Bosch, D., Bruguier, O., 1996. Inherited zircon and titanite U–Pb systems in an Archaean gneiss from southwestern Australia: implications for U–Pb stability of titanite. *Earth and Planetary Science Letters* 141, 187–198.

- Roberts, N.M.W., Spencer, C.J., 2015. The zircon archive of continent formation through time. *Geological Society, London, Special Publications* 389, 197–225.
- Romano, R., Lana, C., Alkmim, F.F., Stevens, G.S., Armstrong, R., 2013. Stabilization of the southern portion of the São Francisco Craton, SE Brazil, through a long-lived period of potassic magmatism. *Precambrian Research* 224, 143–159.
- Rosière, C.A., Spier, C.A., Rios, F.J., Suckau, V.E., 2008. The itabirites from the Quadrilátero Ferrífero and related high-grade ores: an overview. *Reviews in Economic Geology* 15, 223–254.
- Rozel, A.B., Golabek, G.J., Jain, C., Tackley, P.J., Gerya, T., 2017. Continental crust formation on early Earth controlled by intrusive magmatism. *Nature* 545 (7654), 332.
- Sandiford, M., McLaren, S., Neumann, N., 2002. Long-term thermal consequences of the redistribution of heat-producing elements associated with large-scale granitic complexes. *Journal of Metamorphic Geology* 20, 87–98.
- Santos, J.O.S., Hartmann, L.A., Bossi, J., Campal, N., Schipilov, A., Piñeiro, McNaughton, N.J., 2003. Duration of the trans-amazonian cycle and its correlation within south America based on U–Pb SHRIMP geochronology of the La Plata craton, Uruguay. *International Geology Review* 45, 27–48.
- Schaltegger, U., Davies, J.H.F.L., 2017. Petrochronology of zircon and baddeleyite in igneous rocks: reconstructing magmatic processes at high temporal resolution. *Reviews in Mineralogy and Geochemistry* 83 (1), 297–328.
- Seixas, L.A.R., Bardintzeff, J.M., Stevenson, R., Bonin, B., 2013. Petrology of the high-Mg tonalites and dioritic enclaves of the ca. 2130 Ma Alto Maranhão suite: evidence for a major juvenile crustal addition event during the Rhyacian orogenesis, Mineiro Belt, southeast Brazil. *Precambrian Research* 238, 18–41.
- Seixas, L.A.R., David, J., Stevenson, R., 2012. Geochemistry, Nd isotopes and U–Pb geochronology of a 2350 Ma TTG suite, Minas Gerais, Brazil: implications for the crustal evolution of the southern São Francisco craton. *Precambrian Research* 196, 61–80.
- Silver, P.G., Behn, M.D., 2008. Intermittent plate tectonics? *Science* 319, 85–88.
- Shirey, S.B., Hanson, G.N., 1984. Mantle derived Archaean monzodiorites and trachyandesites. *Nature* 310, 222–224.
- Smart, K.A., Tappe, S., Stern, R.A., Webb, S.J., Ashwal, L.D., 2016. Early Archaean tectonics and mantle redox recorded in Witwatersrand diamonds. *Nature Geoscience* 9, 255–259.
- Smithies, R.H., 2000. The Archaean tonalite–trondhjemite–granodiorite (TTG) series is not an analogue of Cenozoic adakite. *Earth and Planetary Science Letters* 182, 115–125.
- Smithies, R.H., Champion, D.C., Van Kranendonk, M.J., 2009. Formation of Paleoproterozoic continental crust through infracrustal melting of enriched basalt. *Earth and Planetary Science Letters* 281, 298–306.
- Spencer, C.J., Kirland, C.L., Taylor, R.J.M., 2016. Strategies towards statistically robust interpretations of in situ U–Pb zircon geochronology. *Geoscience Frontiers* 7, 581–589.
- Stern, R.J., 2005. Evidence from ophiolites, blueschists, and ultrahigh-pressure metamorphic terranes that the modern episode of subduction tectonics began in Neoproterozoic time. *Geology* 33, 557–560.
- Stern, R.J., 2016. Is plate tectonics needed to evolve technological species on exoplanets? *Geoscience Frontiers* 7, 573–580.
- Stern, R.J., Leybourne, M.I., Tsujimori, T., 2016. Kimberlites and the start of plate tectonics. *Geology* 44, 799–802.
- Stern, R.J., Leybourne, M.I., Tsujimori, T., 2017. Kimberlites and the start of plate tectonics - Reply. *Geology* 45, e406. <https://doi.org/10.1130/G38725Y.1>.
- Storey, C.D., Jefferies, T.E., Smith, M., 2006. Common lead-corrected laser ablation ICP–MS U–Pb systematics and geochronology of titanite. *Chemical Geology* 227, 37–52.
- Tarney, J., Jones, C.E., 1994. Trace element geochemistry of orogenic igneous rocks and crustal growth models. *Geological Society of London Journal* 151, 855–868. <https://doi.org/10.1144/gsjgs.151.5.0855>.
- Taylor, S.R., McLennan, S.M., 1985. The Geochemical evolution of the Continental crust. *Reviews of Geophysics* 33, 241–265.
- Teixeira, W., Ávila, C.A., Dussin, I.A., Corrêa Neto, A.V., Bongioiolo, E.M., Santos, J.O.S., Barbosa, N., 2015. Zircon U–Pb–Hf, Nd–Sr constraints and geochemistry of the Resende Costa Orthogneiss and coeval rocks: new clues for a juvenile accretion episode (2.36–2.33 Ga) in the Mineiro belt and its role to the long-lived Minas accretionary orogeny. *Precambrian Research* 256, 148–169.
- Teixeira, W., Ávila, C.A., Dussin, I.A., Vasques, F.S.G., Hollanda, M.H.M., 2012. Geochronologia U–Pb (LA–ICPMS) em zircão detrítico de rochas metassedimentares paleoproterozoicas da parte sul do Craton do São Francisco: proveniência, delimitação temporal e implicações tectônicas. In: 12o Simpósio de Geologia do Sudeste/16o Simpósio de Geologia de MG. Sociedade Brasileira de Geologia, Anais, CDRom, Nova Friburgo, p. 12.
- Teixeira, W., Ávila, C.A., Nunes, L.C., 2008. Nd–Sr isotopic geochemistry and U–Pb geochronology of Fê granitic gneiss and Lajedo granodiorite: implications for Paleoproterozoic evolution of the Mineiro belt, southern São Francisco Craton. *Geologia USP Série Científica* 8, 53–73.
- Teixeira, W., Oliveira, E.P., Marques, L.S., 2017a. The nature and evolution of the Archean crust of the São Francisco craton. In: Heilbron, M., Alkmim, F., Cordani, U.G. (Eds.), *São Francisco Craton, Eastern Brasil: Tectonic Genealogy of a Miniature Continent, Regional Geology Review Series*. Springer-Verlag, pp. 29–56. https://doi.org/10.1007/978-3-319-01715-0_3. Chapter 3.
- Teixeira, W., Oliveira, E.P., Peng, P., Dantas, E.L., Hollanda, M.H., 2017b. U–Pb geochronology of the 2.0 Ga Itapeverica graphite-rich supracrustal succession in the São Francisco Craton: tectonic matches with the North China Craton and paleogeographic inferences. *Precambrian Research* 293, 91–111.
- Toledo, C.L.B., 2002. Evolução geológica das rochas máficas e ultramáficas no Greenstone Belt Barbacena, na região de Nazareno, MG (Unpubl. Doctoral Thesis). Instituto de Geociências, Universidade Estadual de Campinas, UNICAMP, Campinas, 307 pp.
- Vasquez, M.L., Macambira, M.J.B., Armstrong, R.A., 2008. Zircon geochronology of granitoids from the western Bacajá domain, southeastern Amazonian craton, Brazil: Neoproterozoic to Orosirian evolution. *Precambrian Research* 161, 279–302.
- Vervoort, J.D., Kemp, A.I.S., 2016. Clarifying the zircon Hf isotope record of crust–mantle evolution. *Chemical Geology* 425, 65–75.
- Williams, H., Hoffman, P.F., Lewry, J.F., Monger, J.W.H., Rivers, T., 1991. Anatomy of North America: thematic portrayals of the continent. *Tectonophysics* 187, 117–134.
- Woodhead, J.D., Hergt, J.M., Davidson, J.P., Eggins, S.M., 2001. Hafnium isotope evidence for ‘conservative’ element mobility during subduction zone processes. *Earth and Planetary Science Letters* 192, 331–346.